Bioenergy production from pretreated rice straw in Nigeria: An analysis of novel three-stage anaerobic digestion for hydrogen and methane co-generation

Emeka Boniface Ekwenna [a,b,*], Yaodong Wang [a], Anthony Roskilly [a,b]

[a] Department of Engineering, Durham University, Durham DH1 3LE, UK
[b] Durham Energy Institute, Durham University, Durham, DH1 3LE, UK

HIGHLIGHTS

- Co-production of H_2 and CH_2 from PT rice straw in a novel 3-stage digestion process.
- Improving rice straw energy recovery via innovative potash extract pretreatment.
- Daily H_2 and CH_4 yield from RS improved with chemical/PE and enzyme pretreatment.
- NaOH and PE-PT RS digesters generated the highest electricity, thermal, and cooling fluid in CCHP.
- *Firmicutes* and *Euryarchaeota* dominated acidogenic and methanogenic reactors, respectively.

GRAPHICAL ABSTRACT
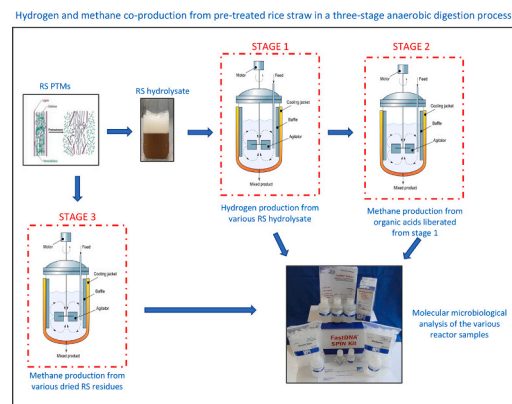
Hydrogen and methane co-production from pre-treated rice straw in a three-stage anaerobic digestion process

ARTICLE INFO

ABSTRACT

The response to Nigeria's energy inadequacies and waste management issues is projected in this research to be achieved with hydrogen and methane co-produced from pretreated (PT) rice straw (RS) in a three-stage digestion process. This study also demonstrated a novel pretreatment (PTM) agent to improve biological energy recovery from RS. The objectives were accomplished using acidogenic and methanogenic procedures in batch, semi-continuous and continuous systems after pretreating RS with chemical/potash extract (PE) followed by a biological agent. At the same time, the energy assessments were done using data from the laboratory study and the literature. The research findings indicated that at the acidogenesis stage, specific hydrogen yield was insignificant when chemical agents and PE were employed alone. However, the daily H_2 production increased when the PT RS residues were enzymatically hydrolysed with NaOH-PT (114 NmL H_2 g^{-1} TS d^{-1}) and PE-PT (103 NmL H_2 g^{-1} TS d^{-1}) RS substrates having the highest values at steady states and raw RS producing the least (30 NmL H_2 g^{-1} TS d^{-1}). In the methanogenesis phase, chemical/ PE PTM followed by enzymatic hydrolysis of RS improved the daily specific methane production by 18%, 31.7% and 41.5% for HCl, PE and NaOH-PT RS residues. The methane production efficiency was 80% for NaOH, 75% for PE, and 68% for HCl RS PT samples, while the raw

RS was 48%. The total output energy expressed in electricity and thermal production using combined cooling, heat, and power (CCHP) showed that NaOH and PE-PT RS digesters gave the highest electricity (892.43 and 852.00 $KWh_{elect.}$ tonne^{-1} TS) and thermal (1194.10 and 1140 $KWh_{therm.}$ tonne^{-1} TS) yield respectively. Similarly, the cooling fluid in KWh_{cool} produced per tonne of TS RS was 835.57, 798.00 and 741.66 for NaOH, PE and HCl PT RS samples. Finally, whereas the *Firmicutes,* especially the *Clostridium*, *Ruminococcus* and *Thermoanaerobacterium,* were the dominant microbial community in acidogenic digestates, the *Euryarchaeota* typified by *Methanobacterium*, *Methanosarcina* and *Methanosaeta* were the principal phyla for most methanogenic reactors.

Nomenclature

AD	Anaerobic digestion
ADS	Activated digested sludge
ASV	Amplicon sequence variant
BGDB	Borosilicate glass Duran bottle (s)
CHP	Combined heat and power
CCHP	Combined cooling, heat, and power
C/N ratio	Carbon-to-nitrogen ratio
COD	Chemical oxygen demand
COP	Cooling coefficient of performance
CSABR	Continuous stirred anaerobic bioreactor
DCS	Digested cattle slurry
DADA	Divisive amplicon deionising algorithm
DM	Digestate Mixture
EPFB	Empty palm fruit bunch
F/M	Food/microbial
FOS	in German *Fluchtige Organische Säuren* (TVFA expressed in mg HAc L^{-1})
FOS: TAC	Ratio of TVFA to total alkalinity
GC	Gas chromatography
GHG	Greenhouse gases
HHV	Higher heating value
HRT	Hydraulic retention time
LCB	lignocellulose biomass
LCBD	Local contribution of beta diversity
LCV	Lower calorific value
LHV	Lower heating value
MPE	Methane production efficiency
Mt	Metric tonnes
Mtoe	Million tonnes of oil equivalent
N mL	Millilitres in normal conditions (gas volumes at 0 °C and an atmospheric pressure of 101.3 kPa)
OLR	Organic loading rate
PCR	polymerase chain reaction
PE	Potash extract
PFOR	Pyruvate: ferredoxin oxidoreductase
PT	Pretreated
PTM	Pretreatment(s)
QIIME	Quantitative Insights into Microbial Ecology
RS	Rice straw
RSC	Reducing sugar concentration
SEM	Scanning electron microscope
SBY	Specific biogas yield
SCFA	short-chain fatty acid (s)
SHP	specific hydrogen production
SHY	specific hydrogen yield
SMP	Specific methane production
SMY	specific methane yield
TAC	in German Totales Anorganisches Carbonate (total alkalinity buffer expressed as mg. L^{-1} of CaCO$_3$.
TBMP	Theoretical biochemical methane potential
TCC	Total carbon content
TCOD	Total chemical oxygen demand
TOC	Total organic carbon
TVFA	Total volatile fatty acid(s)
TS	Total solid
TSS	Total suspended solids
VS	Volatile solids
VSS	Volatile suspended solids
WLP	Wood-Ljungdahl pathway

1. Introduction

Nigeria's energy needs are increasing due to industrialisation and population growth. The predicted energy demand is about 180 GW, while its population is 221 million [75,102]. Although Nigeria is a fossil-dependent country, Nigeria depends on biomass fuels like firewood and wastes as the total primary energy supply [40]. Using firewood and biomass waste has altered the country's vegetation and increased desertification and deforestation, leading to severe flooding and other environmental issues [75,97]. Consequently, the over-reliance on firewood and waste as the primary energy consumption source contributes to greenhouse gases (GHG), notably anthropogenic CH_4, CO_2, CO and NO_x and volatile organic acids [5,57,67]. These gases, especially CH_4 and CO_2, affect the ozone layer and significantly cause climate change. According to the IEA [40], Nigeria's total CO_2 emissions have increased from 28.1 million tonnes (Mt) of CO_2 in 1990 to 88.1 Mt. CO_2 in 2020, with 0.4 t CO_2 emission per capita. Recent estimates by the Global Carbon Atlas [37] suggest that Nigeria's total CO_2 emissions have increased to about 137 Mt. CO_2, indicating a concerning trend of rising GHG emissions in the country.

Traditionally, Nigeria's electricity comes from hydro systems and gas plants, and these systems are archaic, poorly maintained and operated mainly by unsuited professionals [40,70]. As a result, electricity in Nigeria remains within the 6.5 to 8.2 GW capacity range, which is insufficient for the country [34,73,74]. Therefore, energy from fossil sources has been utilised for many years to satisfy these demands. However, the most striking debate in the power and the environmental sector is clean energy generation due to rising atmospheric carbon emissions from fossil-based energy sources [36]. Alternative renewable energy technologies such as wind, hydro, solar, geothermal, and oceanic are not without issues as they are capital intensive. Hence, various ways of generating energy from cheap and renewable sources are being researched and developed. There has been growing interest in biomass anaerobic digestion (AD) technology as the most promising renewable energy technology. The near carbon neutrality of biomass, cheap availability of biomass materials globally and the solution to environmental problems covey biomass as a good energy source for the future [24,41]. Nigeria has about 20–21 million cattle [32] and produces about 0.59 Mt. of cattle slurry daily and about 215 Mt. of cattle slurry annually. In addition, Nigeria currently produces around 14.1 Mt. of RS per year [32]. These agricultural wastes can be harnessed to produce energy products using the AD process and solve numerous environmental

pollution problems. The high heating value (HHV) of RS ranges from 14.02 to 15.03 MJ kg^{-1}, with low heating value (LHV) values around 13 and 13.9 MJ kg^{-1} [15,62,71]. These energy values are typical examples of the energy contribution of RS.

Conventional biogas processes have long focused on methane production. Nevertheless, in recent years, the research and development of hydrogen have increased due to the positive attributes of hydrogen as an alternative energy carrier. High energy content and efficiency, and environmentally friendly production are the reasons hydrogen is the energy of the future [14,31,46]. In terms of energy yield per molecule, hydrogen is high, with a calorific value of 142 KJ g^{-1} [14,27,31]. Hydrogen can be traditionally produced in several ways, such as steam reformation of natural gas and fatty oils, gasification of heavy hydrocarbons or coal or biomass, and nuclear and renewable electrolysis [36,46,85]. Nonetheless, the hydrogen of the future is best produced biologically to mitigate problems associated with physical and chemical approaches. Among other biological means, hydrogen is generated during the acidogenic stage in an AD process of methane production [17,18].

On the other hand, methane is a combustible gas produced by thermochemical, catalytic, and biological processes. The catalytic process is commonly called the Sabatier process and usually involves reacting hydrogen with carbon monoxide or carbon dioxide at higher temperatures between 500 and 600 °C under nickel catalysis [12]. In the biological process, methane-rich biogas is produced anaerobically by the breakdown of biomass (crop and plant debris, energy groups, animal manure, agricultural waste, municipal solid waste) using AD technology. Typically, biogas generated from the AD process contains about 55 to 70% CH$_4$ [66], and this component, methane (also a major component of natural gas), provides the calorific value. Besides being an energy resource, methane is also a greenhouse gas, 21 times by weight the global warming potential of CO$_2$ [12].

Despite the benefits of AD to produce hydrogen and methane, the digestion of RS for biogas production is limited by the low digestibility of its fibre content [28,29,57,100] and its high ash content of 15–20% [63]. It is said that without the pretreatment (PTM) of lignocellulose biomass, only 20% of the hypothetical maximum sugar can be obtained from enzymatic hydrolysis [28,106]. Therefore, effective PTMs are required to break the complex and heterogeneous matrices, increase biomass surface area, and create micropores on lignocellulose materials to improve enzyme accessibility, hydrolysis, and cellulose degradation [18,28,29,46]. There have been several works on RS PTMs for improving acidogenic and methanogenic processes by Lo et al. [60], Chang et al. [22], He et al. [38], Liu et al. [59], Sen et al. [90], Mustafa et al. *[68]*, Dong et al. [28,29], Kainthola et al., [42], Kannah et al., [43] Balachandar et al., [13], Srivastava et al. [91], Cai et al. [18], Kim et al. [46] and Li et al. [57]. Nonetheless, the PTM of lignocellulose biomass invariable increases biogas production cost and presents environmental hazards. Hence, environmentally friendly, and cost-effective lignocellulose PTM methods are being investigated. Thus, in this research, potash extract (PE), as a PTM agent, was explored as a chemical substitute for the PTM of lignocellulose. This ingenious hypothesis is on the basis that PE is alkaline and contains varying metallic cations and anions [111] that may affect the physiology of the lignin components of lignocellulose biomass (LCB), similar to structural effects produced by an alkali PTM on LCB [46,87]. The potash is produced locally in Nigeria as leftover ash from the controlled use of empty palm fruit bunches (EPFB) as a heat energy source for cooking.

Furthermore, a *three-stage* anaerobic digestion *process* that produces hydrogen and methane from RS co-digested with digested cattle slurry (DCS) is proposed to maximise the energy value of RS. In this innovative three-stage process, the RS hydrolysates are converted into hydrogen, carbon dioxide, and short-chain fatty acids (SCFA) by acidogenic microorganisms in a separate reactor operating at acidic pH. Simultaneously, the hydrolysed RS residues are washed off, dried, and stored for future use in methane production. The hydrogen produced in the first stage is collected using a gas bag, while the SCFA enters the second stage, where they are converted into methane and carbon dioxide. Methane production from the PT RS residues occurs in the third and final stage. Slow-growing methanogens are preferred to achieve optimal results in the second and third stages, operating under neutral pH with longer HRT (7–30 d). The *three-stage* anaerobic digestion process is categorised based on the reactants (feedstock) rather than the traditional products typical of the two-stage AD process. The main difference between the two and *three-stage* hydrogen and methane production processes is that while hydrogen production processes are optimised, RS residues are further broken down to methane in the latter process. Therefore, energy is maximised and recovered from the RS substrates.

Although there is much literature on individual hydrogen production, which involves the breaking down of sugars to H$_2$ and CO$_2$ during the acidogenesis stage of an AD process [7,13,18,22,23,28,29, 38,43,46,52,55,59,60,79,83,89,91] as well as single-stage methane production process that convert C$_1$ methylated compounds, acetate and H$_2$/ CO$_2$ to CH$_4$ mainly by the *Archaea* in an anorexic environment [42,57,68,99,104], there are relatively few reports on the two-stage production processes where H$_2$ and CH$_4$ is co-produced during the digestion process [8,9,47,53,69,78,95,103,109]. However, to the writer's knowledge, there are no documented three-stage *reactants* processes. Therefore, the objectives of this study are to a) investigate the co-production of hydrogen and methane from chemical/PE-PT enzymatically-enhanced RS in a unique and inventive *three-stage* AD process; b) establish the mass balance of the RS digestion processes; c) calculate and compare the various energy values of the biogas generated from the three-stages using the CCHP strategy and finally d) analyse the microbial community composition of the fermentation and the digestion processes.

2. Materials and methods

2.1. Rice straw collection and preparation

The RS used in this study was collected from Xiamen University, China and was used as feedstock. First, the RS was chopped into 2 mm pieces and washed thoroughly 3 times with tap water before placing it in an electric oven at 70 °C until dry. Next, the sized-medium RS was milled with a grinder, sieved through 750 μm and stored in a sealed plastic container at room temperature until use. The composition of RS (dry basis) was determined to be 39.5% cellulose, 30.5% hemicellulose, 17% lignin and 13% others.

2.2. Potash collection and preparation of potash extract

The ash (potash) from empty palm fruit was collected from a mound of burnt empty palm bunches at a palm oil processing plant in Anara town, Imo State, Nigeria. Potash extract (PE) was made by mixing 500 g of potash with 1 L of deionised water in a ratio of 1:2. The mixture was stirred correctly and allowed to stand at room temperature for 48 h. After, the potash mixture was vacuum filtered using Whatman filter paper (0.45 μm). The residue was then rinsed with 500 mL of distilled water to give a potash-to-distilled water ratio of 1:3. The filtrate pH value was 11.05 ± 0.25, which is strongly alkaline. The colour of the PE was found to be dark brown, and then the PE was stored at a cooling temperature of 4 °C. Before use, the metal analysis was carried out (Table 1).

2.3. Seed sludge collection and preparation

The seed sludge was activated digested slurry (ADS) and DCS. They were obtained from Cockle Park Farm, Newcastle University, Newcastle Upon Tyne, UK, where cattle and pig manure are processed and stored at refrigerating temperature until future application. Before use, the sludge was degassed to remove any remaining indigenous biomass by incubating it for 30 days at 37 or 55 °C.

Table 1
Elemental composition of potash, RS, ADS and DCS.

Cations	Potash (mg g^{-1})	RS (mg g^{-1})	ADS (mg L^{-1})	Raw DCS (mg L^{-1})
Calcium	557.50	45.30	208.65	204.15
Magnesium	346.42	3.48	206.88	199.0.78
Sodium	280.22	2.22	66.22	76.42
Potassium	5041.55	119.35	375.08	345.88
Zinc	4.37	0.36	2.97	2.15
Nickel	0.29	9.27	0.20	1.20
Aluminium	113.45	1.15	21.95	15.77
Iron	113.18	47.89	131.37	135.13
Manganese	16.37	5.56	5.26	5.26
Copper	10.35	0.26	3.11	3.75
Lead	<0.05	<0.05	<0.05	<0.05
Silicon	81.32	10.87	1.21	1.00
Arsenic	0.16	0.05	1.10	0.56
Chromium	0.23	0.21	0.29	1.29
Strontium	0.13	0.09	3.74	2.99
Barium	0.70	0.28	0.47	0.50
Selenium	1.58	0.2	0.71	0.67
Anions				
Chloride	366.80	NA	NA	NA
Nitrite	16.90	NA	NA	NA
Bromide	4.43	NA	NA	NA
Sulphur	137.50	NA	27.09	25.00
Nitrate	1.25	NA	NA	NA
Phosphor	201.50	15.01	NA	NA

NA: Not available.

The seed sludge metal analysis (Table 1) and physicochemical attributes and solid analysis applied in the anaerobic digestion are characterised in Table 2.

2.4. Chemical pretreatment of RS

2.4.1. Acid, base, and potash extract pretreatment of RS

A modified method of Zhang and Cai [105] was employed to prepare HCl-PT RS samples. About 100 g of milled RS was added to a conical flask containing 400 mL of 1 M hydrochloric acid to maintain the solid-to-liquid ratio at 1:4. The mixture was then heated at 100 °C for 1 h. The RS mixture was filtered with 0.2 μm filter paper, and the RS residue was washed thoroughly with distilled water until a neutral pH was achieved. The filtrates were diluted to 6.0 ± 0.2 with 5 M of NaOH, detoxified by lime treatment, and stored at −20 °C until use. The same protocol was followed for NaOH and PE PTMs, with 2% NaOH and 400 mL of PE used for the respective procedures. However, the filtrates were diluted to 6.0 ± 0.2 with 5 M HCl. The salt precipitates were also filtered, as aforementioned. Finally, the RS residue was dried in an oven at 70 °C for 24 h and kept at RT for subsequent use.

Table 2
Physicochemical properties of raw RS and seed sludge.

Analysis	RS	ADS	DCS
TS (g mL^{-1})	0.938	0.016	0.095
TSS (g mL^{-1})	ND	0.013	0.069
VS (g mL^{-1})	0.815	0.009	0.073
VSS (g mL^{-1})	ND	0.008	0.0052
Ash (g mL^{-1})	0.123	0.007	0.0022
VS (%)	87	56	77
Ash (%)	13	44	23
Carbon (%)	42.76	34.22	38.54
Nitrogen (%)	0.68	2.92	2.98
Hydrogen (%)	6.3	3.77	3.99
C/N ratio	ND	11.7	12.9
NH$_4^+$-N (g mL^{-1})	ND	0.23	0.27
Moisture Content (%)	3	97	95
Alkalinity (mg CaCO$_3$ L^{-1})	ND	5280	4010

ND: Not determined.

The chemical PTMs were done in triplicates, and the mean values were presented, while the controls were also prepared without the respective PT agents following the same protocol.

2.4.1.1. Detoxification of HCl-PT RS filtrate. The Palmqvist and Hahn-Hagerdal [76] protocol was employed during the detoxification of HCl-PT RS filtrate. The pH value of the RS PT filtrate was initially adjusted to 10.0 ± 0.1 by adding Ca (OH)$_2$ and was agitated for an hour. The pH value of this solution was then adjusted to 5.5 ± 0.1 by adding H$_2$SO$_4$ (1 N). Next, the sediments were removed, and activated carbon (1.5% w/v) was added to the supernatants. The mixture was stirred for an hour. The supernatant was then collected and stored at −20 °C for future use in hydrogen production.

2.5. Lignin determination test

Zhao et al. [108] modified method was used in the delignification analysis. About 500 mg of PT RS residue and untreated RS (200 μm) were placed in a 100 mL flask containing 35 mL of distilled water and then heated in a water bath at 80 °C. After about 30 min, a mixture of 0.5 g of sodium chloride and 0.1 mL of acetic acid (100%) was added to the mix every hour thrice. The mixtures were filtered with a Buchner funnel, and the residue was rinsed with distilled water. Finally, the RS residues were dried at 105 °C for 24 h to determine their weight. The weight loss is considered as lignin content.

2.6. Enzymatic hydrolysis of PT RS residues

The cellulase enzyme was assumed to be isolated and optimised from the soil using the protocol of Acharya et al. [1,2] and Kshirsagar et al. [49]. However, for this study, dried PT RS residues from chemical PTMs were enzymatically hydrolysed after solids analysis (Table 3) using cellulase (0.8 U mg^{-1}) (SIGMA) in 0.05 M sodium citrate buffer at 5% (*w/v*) PT RS on a rotary shaker at 150 rpm for 5 days. The hydrolysis temperature was maintained at 37 °C while the pH of the buffer was 4.95 ± 0.4. After the enzymatic-process period, the hydrolysis reaction was stopped by heating at 100 °C for 20 min. The cellulase enzyme was loaded at a different concentration to obtain the best enzymatic hydrolysis condition for sugar production, and samples were taken every 24 h for sugar concentration analysis. The enzymatic hydrolysis reaction was done in triplicate, and the average result was presented. The hydrolysates were stored at −20 °C until use for sugar analysis and hydrogen fermentation. Simultaneously, the various RS enzymatic residues (HCl-PT RS, NaOH-PT RS and PE-PT RS) were thoroughly washed, dried, and stored in a zip-lock back at RT until use. One unit of cellulase activity was defined as 1.0 μg of reducing sugar equivalent released per min. Finally, the enzymatic conversion rates of the different PT RS residues were obtained as the percentage difference from the original sample before hydrolysis and after hydrolysis.

2.7. Hydrogen fermentation process (stage 1 process)

2.7.1. Batch fermentation process

The acidogenesis setup is outlined in Table 4 and detailed as follows. Batch cultures were performed using a 500 mL borosilicate glass Duran

Table 3
Characterisation of some PT RS residues and untreated RS.

PT-RS Samples	Calculated DM (TS) Content (%)	Calculated DM (VS) Content (%)	Ash (%)
HCl-PT RS	98	90	8
PE-PT RS	94	88	6
NaOH-PT RS	96	89	7
Solid PE-PT	92	84	8
Solid NaOH-PT	96	89	7
Untreated	95	82	13

Table 4
Operational parameters of hydrogen and methane fermentation processes.

Operational Parameter	Hydrogen fermentation bioreactor (Stage 1)	
	Batch	CSABR
HRT	4 days	40 days
Substrate Type	PT RS hydrolysates	PT RS hydrolysates
OLR	–	1.0 gCOD sugar L^{-1} added day $^{-1}$
F/M	0.75	0.75
pH	5.5	5.5
Reactor size	500 mL	1 L
Temperature	55 °C	55 °C
	Methane fermentation bioreactor (Stage 2)	
	Fed-batch	CSABR
HRT	30 days (3 HRT)	40 days
Substrate Type	VFA	VFA
OLR	1.0 gCOD L^{-1}	1.0 gCOD L^{-1} added day $^{-1}$
F/M	0.4	0.4
pH	7	7
Reactor size	1 L	1 L
Temperature	37 °C	37 °C
	Methane fermentation bioreactor (Stage 3)	
	Batch	CSABR
HRT/SRT	30 days	60 days
Substrate Type	PT RS residues	PT RS residues
OLR	–	1 gTS RS L^{-1} added day $^{-1}$
F/M	0.4	0.4
pH	6.9	6.9
Reactor size	500 mL	5 L
Temperature	37 °C	37 °C

bottle (BGDB) (VWR 215–1594) with a working volume of 400 mL and a food/microbial (F/M) ratio of 0.75. The bioreactors were identified throughout the study as HCl, PE and NaOH-PT RS, reflecting their respective RS substrates. The untreated RS was labelled as raw RS. Hydrogen fermentations were done in triplicates in an automated stirred incubator system (Fig. 1a) with an initial pH of 5.8 ± 0.2. However, 5 M HCl and 5 M NaOH were used to maintain an active pH of 5.5 ± 0.1. The operating temperature of the incubator system was 55 °C, and the rotational speed was kept at 120 rpm. The reactor mixture was augmented with a 5% mineral medium. The mineral medium contained per litre: (Nhydrolysed2 g; KH_2PO_4 0.125 g; Na_2HPO_3 5.24 g $CaCl_2$ 0.3 g;

$MgCl_2 \cdot 4H_2O$ 0.1 g; $FeSO_4 \cdot 7H_2O$ 0.025 g; $CoCl_2 \cdot 6H_2O$ 0.0001 g; $ZnSO_4 \cdot 7H_2O$ 0.0024 g; $CuSO_4 \cdot 5H_2O$ 0.005 g, peptone 0.75 g, and distilled water 1000 mL. Chemically and enzymatically-PT RS hydrolysates were used as media for the 4-day incubation. The reactors were purged with nitrogen for 3 min, and the daily biogas was collected in a 500 mL SupelTM-Inert Multi-Layer Foil Gas Sampling Bag equipped with a screw cap valve (SCV) connected to the syringe gas take-off of the reactors through PVC tube. The total biogas volume produced by each fermenter was measured daily, and the hydrogen concentration (%) was determined using a thermal conductivity detector gas chromatography-Trace GC Ultra (Thermo Scientific, UK) with argon as the carrier gas and calculated with Verein Deutscher Ingenieure (VDI) 4630 [98].

2.7.2. Continuous fermentation procedure

After the batch hydrogen fermentation using the PT RS hydrolysates as substrates, the hydrogen production was switched to a continuous process in a continuous stirred anaerobic bioreactor (CSABR) using the same feedstock. The CSABR setup (Fig. 1b) has 8 Quickfit® glass anaerobic bioreactors, each with a 1-L capacity consisting mainly of the gas inlet/outlet system, the feeding mechanism and stirrers that are controlled automatically by an adjustable electric motor. A working volume of 900 mL was employed, and the bioreactors were incubated in a water-filled bath at 55 °C using an automatic heating system (Grant, T100). This temperature was also sustained by covering the top of the water bath with spongy-like foams. The cultivation was done in duplicates at the same conditions as the batch hydrogen fermentation Section 2.7.1. The CSABR was seeded with heat-shocked and acclimatised DCS sludge to commence the digestion process, while the headspace of the individual bioreactors was flushed with nitrogen for 5 min to provide an oxygen-free condition. After reactivating the inoculum inside the bioreactors, the continuous fermentation was operated at an organic loading rate (OLR) of 1.0 gCOD L^{-1} added day $^{-1}$ (Table 4). The fermentation lasted 40 days duration after steady-state conditions were achieved. The steady-state involves the daily draining of about 10% (reactor working volume) of the digestate from the feeding outlet using a germ-free syringe and replacing it with the same fresh medium consisting of the RS PT hydrolysate, ammonium nitrogen carbonate (10 g

Fig. 1. Fermenters employed for the different anaerobic digestion studies with gas and feeding outlets, a) batch mode (500 mL) in an automated stirred incubator system and continuous system (CSABR) b) 1 L and c) 5 L.

L^{-1}) and water. Each reactor was connected to a 500 mL Supel™-Inert Multi-Layer Foil gas bag for biogas collections, and the total biogas volume produced by each CSABR was measured daily. The hydrogen content (%) was analysed as described in Section 2.7.1.

2.8. Methane production process (stage 2 and 3 processes)

2.8.1. Utilisation of effluents (organic acids) for methane production (Stage 2)

The withdrawn effluents from the continuous reactor for hydrogen fermentation and the PT RS residue were used to produce methane. The seed sludge employed was obtained from an active methane-producing sludge (ADS) and adapted as stated in Section 2.3. The methane digestion process was defined in two stages. a) In the *stage 2* process, the fed-batch mode was employed to produce methane using SCFA produced from Section 2.7 as substrate. Whereas the fed-batch procedure was the same as described in Section 2.7.1 with variations in cultivation condition, the CSABR setup (Fig. 1b) and cultivation were as described in Section 2.7.2 with differences in operational pH, culture temperature and F/M ratio. The methanogenesis processes for both systems are detailed in Table 4. In the fed-batch system, the feeding was performed every 10 days for 3 times with an OLR of 1.0 gCOD L^{-1} before switching the reactor to continuous mode via the CSABR system (Fig. 1b) for 40 days with VFA fed at 1.0 gCOD L^{-1} added d^{-1}.

The COD removal was calculated using Eq. 1, while a specific volume of the reactor supernatant was removed and replaced with the same amount of fresh effluents (TVFA) in the respective digesters from the *stage 1* continuous anaerobic fermentation process (Section 2.7.2). The biogas collection and CH$_4$ content analysis are detailed in the previous Section.

$$COD\ removal\ (\%) = \frac{COD_A \times VOL_{IN} - COD_B \times VOL_{OUT}}{COD_A \times VOL_{IN}} * 100 \qquad (1)$$

Where COD$_A$ is the COD of the effluent feeding, the VOL$_{IN}$ is the volume of effluent going in, COD$_B$ is the COD of the supernatant withdrawn from the methanogenic reactor, and VOL$_{OUT}$ is the volume of supernatant withdrawn from the methanogenic reactor.

2.8.2. Methane production employing pretreated RS residues as substrates (stage 3)

In contrast, b) in the *stage 3* process, batch and continuous systems were employed for methane production using the different RS PT residues as feedstock (Table 4). A one-step AD procedure for methanogenesis was also performed with untreated RS for comparative purposes. Stage 3 batch cultivations were done in triplicates as defined in Section 2.8.1 and Table 4. On the other hand, the CSABR setup (Fig. 1c) and cultivation were described in Section 2.7.2 but with differences in the cultivational parameters as detailed in Table 4. At pseudo-steady-state, the reactors were fed 1 gTS L^{-1} added d^{-1} of PT RS residues for 60 d. The alkalinity of the systems was sustained at FOS/TAC (*Fluchtige Organische Sauren* (mg HAc L^{-1})/ *Totales Anoranisches Carbonate* (mg L^{-1} CaCO$_3$) ratio 0.2–0.28, which was calculated by titrating the weekly effluents to pH 5.75 for partial alkalinity (PA) and pH 4.3 for intermediate alkalinity (IA) [61]. The bicarbonate alkalinity (BA), the same as the PA, is corrected using Eq. 2.

$$BA = [TA - (0.85 \times 0.83 \times TVFA)] \qquad (2)$$

Where BA is the bicarbonate alkalinity in mg L^{-1} CaCO$_3$, TA is the total alkalinity measured in mg L^{-1} CaCO$_3$, and TVFA is the total volatile fatty acids in mg HAc L^{-1}. Thus, the numbers 0.85 and 0.83 are correction factors that consider 85% of ionisation of the acids to the titration endpoint and acetic acid into alkalinity.

Each reactor was connected to a 1 L Supel™-Inert Multi-Layer Foil gas bag for daily gas sampling, while the total biogas volumes produced by each CSABR were measured daily. Finally, the methane content (%) was determined using Carlo Erba HRGC 5160 GC equipped with a flame

ionisation detector with helium as the carrier gas and corrected with VDI 4630 [98]. At the end of the experiment, the digestates from the various PT RS residue reactors were separated by centrifugation at 5000 *g* for 15 min, dried at 80 °C for 24 h and stored at RT, while the degree of degradation or percentage TS RS reduction calculated using Eq. 3.

$$TS_{red} = \frac{Q_{in} * TS_{in} - Q_r * TS_r}{Q_{in} * TS_{in}} * 100 \qquad (3)$$

Where Q$_{in}$ is the flow into the reactor, Q$_r$ is the flow out of the reactor, TS$_{in}$ is the TS content in the incoming substrates, and TS$_r$ is the TS content in the effluent.

2.9. Energy value, electricity, and thermal generation from pretreated RS samples

The biogas yields (hydrogen and methane) of all the stages in this study were used to calculate the lower calorific value (LCV) from the hydrolysates and residues of different PT RS. The energy yields were estimated in kg and a tonne of RS per weight for biogas and 99% pure hydrogen and methane (Tables 7–4). The biogas therein is considered a mixture of H$_2$ and CO$_2$ or CH$_4$ and CO$_2$, while the energy value was presented in KJ kg^{-1} instead of KJ m^{-3} using the densities of hydrogen and methane gas of 0.09 mg mL^{-1} and 0.716 mg mL^{-1}, respectively. From the energy yield, the corresponding electricity and thermal yield were calculated using the conversion factors listed in Table 5.

2.10. Molecular microbiological analysis

The digestate samples were taken after the completion of each stage procedure and preserved at −20 °C in a sterile 50 mL centrifuge tube for DNA extraction and purification, PCR amplification, and genomic sequencing. A detailed outline is contained in the previous study by Tabraiz et al. [94]. After the Illumina MiSeq sequenced each sample, the resulting raw data (FastQ files) were denoised and quality filtered using Divisive Amplicon Deionising Algorithm (DADA) 2 [19,20] to identify the unique amplicon sequence variants (ASV) from redundant sequences present in the data set. Whereas the chimeric sequences from each sample were removed from each sequence, the non-chimeric sequences from the samples were taxonomically allocated employing the MIDAS 2.0 reference database [19,86,94] in the Quantitative Insights Into Microbial Ecology (QIIME2) pipeline (https://qiime2.org/ [21]. A feature table was then generated for data visualisation and statistical evaluation, containing the unique ASVs and their relative abundance for each sequenced DNA digestate sample. Finally, the statistical analysis, including the Local Contribution of Beta Diversity (LCBD), was conducted on these data to generate figures and pictographs using the MicrobiomeSeq in R packages [92].

2.11. Measurement of lignocellulose composition of RS

The cellulose, hemicellulose, lignin, and ash components of the RS were determined using the method reported by Lo et al. [60].

Table 5
Data for calculation of energy equivalents, electricity, and thermal yield.

Reference	Unit	Value	Calorific value	% Purity
1kWh	MJ.	3.6		
1m^3 of methane (enriched)	kWh	9.97		99
1m^3 of methane (biogas)	kWh	6.94		70
1m^3 of methane	MJ.	36	Lcv	99
1m^3 of biogas	MJ.	25	Lcv	70
1m^3 of hydrogen	MJ	10.88	Lcv	99
1m^3 of hydrogen (biogas)	MJ.	5.98	Lcv	55
CHP efficiency $_{elect.}$	%	33–38		
CHP efficiency $_{therm}$	%	45–50		

Data extracted from Pöschl et al. [80] and Präger et al. [81].

Approximately 10 mg of completely dried RS was placed in test tubes containing 1 μL of 72% (*w*/*w*) sulphuric acid. The reaction mixtures were stirred continuously using a glass rod in an ice-cold water bath, then transferred to a water bath set at 30 °C and continuous stirring for 1 h. Subsequently, the acid hydrolysis reactions were ended by placing the tubes in an ice-cold water bath. Next, the sulphuric acid in the tubes was diluted to 4% by transferring all the supernatants to 125 mL serum bottles containing 84 mL of distilled water while the solid residues were rinsed with 50 mL deionised water and used for lignin and ash analysis. The diluted solutions were well mixed, and 1 mL was transferred to anaerobic pressure bottles. The bottles were autoclaved at 121 °C for 1.0 h; afterwards, the hydrolysates were collected and neutralised to pH 6.0 ± 0.2 using calcium carbonate. Later, the concentrations of pentose (hemicellulose) and hexose (cellulose) sugars were measured using HPLC (Shimadzu LC-10AT Liquid Chromatography, equipped with a COREGEL 87H3, and refractory index detector, RID) at 37 with C. 0.005 N of sulphuric used as the carrier phase at a flow rate of 0.6 mL min^{-1}. Finally, the solid residues containing the lignin plus ash were thoroughly dried and recorded as W_A. Subsequently, the dried solid residues were placed in a furnace at 550 °C for 24 h and registered as W_B. The difference between W_A and W_B was the lignin content, while W_B was the ash content.

2.12. Determination of the elemental composition of RS, PE, and biomass samples

The procedure was executed according to the amended report by Nielsen [72]. The wet ash process involves the digestion of 1 g of a dried-powdered sample of RS biomass and 1 mL of seed sludge in a conical flask placed in a fume cupboard. About 10 mL of each of the concentrated H_2SO_4 and HNO_3 acids were poured into the flasks. The biomass and acid mixtures were placed on a hot plate and heated at 120 °C for 15 min. During this heating process, foaming occurred along with the release of NO_2 gas, represented by reddish-brown gas formation. By adding more acids, the digestion process continues until all the biomass is entirely digested, recognised by the appearance of a light-yellow solution. No further NO_2 gas release at this point. The digest was subsequently transferred to a 50 mL standard volumetric flask and was made up to 50 mL with deionised water. A sample of this diluted solution and a PE sample were used to determine the elemental composition using an inductively coupled plasma atomic emission spectrometer (Vista-MPX) equipped with a CCD detector, Newcastle University, UK. The elemental analysis (cations) was performed according to the analytical process outlined in the Standard Methods for the Examination of Water and Wastewater 20th Edition (APHA 3120C) [11]. In contrast, the anionic composition of the PE sample was analysed using HPLC stated in Section 3.1.

2.13. Analytical determination of carbon, hydrogen, nitrogen, oxygen and Sulphur content in RS and seed sludge

The carbon, hydrogen, nitrogen, and sulphur contents of the sludge and RS were analysed from 1 g of the individual biomass using the Perkin-Elmer 2400 CHNS Elemental Analyzer, Newcastle University, UK. The oxygen content of each biomass in the same quantity was measured using Thermo Elemental Analyzer (NA 2000) by Elemental Microanalysis Laboratory, UK. The data (%) obtained were measured to an accuracy of ± 0.1 (Table 6) and were used in producing the stoichiometric formula for RS using the modified Buswell equation (Eq. 4). Whereas the constants "*a, b, c, d* and *e*" were obtained by dividing their various corresponding elements (%) from Table 6 by their molar mass, the molar ratios which gave the chemical formula of RS were achieved by dividing the individual constants with the least constant value. The values of RS ultimate analysis were also used to calculate theoretical biochemical methane potential (TBMP) using Eq. 5 [3].

$$C_aH_bO_cN_dS_e + \left(a - \frac{b}{4} - \frac{c}{2} + \frac{3d}{4} + \frac{e}{2}\right)H_2O \rightarrow \left(\frac{a}{2} + \frac{b}{8} - \frac{c}{4} - \frac{3d}{8} - \frac{e}{4}\right)CH_4$$
$$+ \left(\frac{a}{2} - \frac{b}{8} + \frac{c}{4} + \frac{3d}{8} + \frac{e}{4}\right)CO_2 + dNH_3 + eH_2S \tag{4}$$

$$\text{TBMP} \left(\text{NmL CH}_4 \text{ g VS}^{-1}\right) = \frac{22.4 * \left(\frac{a}{2} + \frac{b}{8} - \frac{c}{4} - \frac{3d}{8} - \frac{e}{4}\right)}{12.017a + 1.0079b + 15.999c + 14.0067d + 32.065e} \tag{5}$$
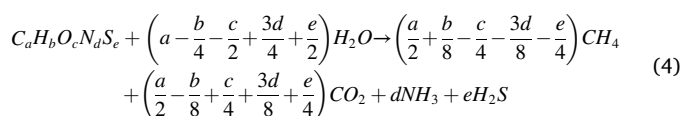
2.14. Determination of RS energy value

The HHV of untreated RS and RS digestates was determined using Oxygen Bomb Calorimeter Parr 1341, Newcastle University, UK. About 0.50 g of the respective samples were measured, pelletised, and placed on the combustion crucible of the bomb head, held by the electrodes containing about 10 cm of a nichrome fuse wire. The ignition wire was then carefully wrapped around the electrode to avoid touching the combustion crucible and form a loop into it and above the pellets. Next, the bomb head was cautiously placed on the bomb cylinder supported by the bomb bracket. The bomb cylinder was screwed tightly after adding a few drops of distilled water from the calorimeter bucket. The bucket contains a specified amount (1600 mL) of distilled water employed in the experiment. The bomb is then pressurised at 30 atm with oxygen gas and carefully submerged in a round-bottomed calorimeter bucket in an insulated container. After confirming a stream of continuous gas bubbles, the electrodes were inserted into the terminal sockets of the bomb. A lid with a stirrer was then used to cover the calorimeter, and the stirrer rotated to ascertain that it was running freely before the drive belt was attached to the pulleys. Following this, the temperature sensor attached to the data logger was inserted into the port on the cover lid. Finally, after igniting the switch, the data produced is recorded via a Pico PT-104

Table 6
Ultimate analysis of RS and seed sludge (ADS and DCS).

Biomass	Carbon (%)	Hydrogen (%)	Nitrogen (%)	Oxygen (%)	Sulphur (%)	Others (%)	C/N ratio
RS	42.76	6.30	0.68	44.70	0.15	5.56	63:1
ADS	34.44	3.77	2.98	NA	0.58	NA	12:1
DCS	38.54	3.99	2.92	NA	0.65	NA	13:1

NA: Not available.

(PT100) data logger connected to a computer. The exact process was first performed using benzoic acid with a known heat of combustion of -26.454 KJ g^{-1} to determine the heat capacity of the calorimeter (C_{cal}) from Eq. 6. The heat of combustion (HHV)) rounded up to MJ kg^{-1} of RS was also calculated using Eqs. 6 and 7. At the same time, the HHV was converted to LHV in MJ kg^{-1} using Eq. 8 [71].

The heat released on combustion of (pellets sample + ignition wire) = Heat absorbed by (water + calorimeter), which is the same as

$$\Delta_c H^0 m_s + \varepsilon = m_w C_{H_2O} \Delta T + C_{cal} \Delta T \qquad (6)$$

Which can be re-written as

$$\Delta_c H^0 = \frac{(m_w C_{H_2O} \Delta T + C_{cal} \Delta T) - \varepsilon}{m_s} \qquad (7)$$

Where,

$\Delta_c H^0$: is the heat combustion of the sample (KJ g^{-1})

m_s: is the mass of the sample (g)

ε: is the heat of combustion of the wire (-9.6 J cm^{-1}) and the length of burnt nichrome wire (cm)

m_w: is the mass of water (g)

C_{H_2O}: is the specific heat capacity of water (4.184 J g ^{0}C^{-1})

C_{cal}: is the heat capacity of the calorimeter (J g ^{0}C^{-1})

ΔT: is the temperature difference ($°C$)

$$LHV = HHV - 0212*H - 0.0245*M - 0.008*Y \ (\text{MJ kg}^{-1}) \qquad (8)$$

Where H, M, and Y are the percentages of hydrogen, moisture, and oxygen from RS, respectively.

2.15. Samples analysis and measurements

The biomass solids, the nitrogen content, the alkalinity, and the chemical oxygen demand were determined by employing standard methods 2540 B, 2320, 4500 and 5220 B, respectively [11], while the concentration of VFA metabolites, such as acetate, butyrate, formate and propionate were measured using an HPLC Thermo-scientific DIONEX AQUION equipped with a Dionex IonPac™ ICE-ASI columns. Furthermore, whereas the reducing sugar concentrations (glucose) from RS enzymatic hydrolysis were measured using the 3, 5 – dintrosalicilic acid (DNS) colourimetry method, the total organic carbon was analysed using a Total Organic Carbon (TOC) Analyzer (TOC-5050A SHIMADZU). Finally, the microstructure of the PT RS residues and raw RS were observed using a scanning electron microscope (SEM) HITACHI NEXUS, Newcastle University, UK.

2.16. Kinetic and statistical analyses

The kinetic model for biogas (H$_2$ and CH$_4$) production rate and yields were determined using a modified Gompertz equation (Eq. 9) and Matlab software (MATLAB R2016a). At the same time, the data were analysed using statistical Excel software (Microsoft Corporation, USA). As discussed above, the R software packages (R version 3.3.2) were employed for the statistical microbial analysis. The values presented were based on a 5% statistical significance level, and results were shown within ± 2 SD.

$$A(t) = P.exp\left\{ -exp\left[\frac{R_m*e}{P} (\lambda - t) + 1 \right] \right\} \qquad (9)$$

Where A (t) is the cumulative H$_2$ or CH$_4$ production (mL gVS^{-1}); P is the H$_2$ or CH$_4$ production potential (mL gVS^{-1}): R$_m$ is the maximum H$_2$ or CH$_4$ production rate (mL gVS^{-1} d^{-1}); e is 2.71828; λ is the lag phase time (d), and t is the fermentation time (d).

3. Results and discussion

3.1. Characterisation of chemically-PT RS samples and filtrates

3.1.1. Effect of chemical PTMs and delignification of RS

The utmost limitation in applying RS to biological hydrogen production is the solubilisation of the carbon content. Since hydrogen is produced at the acidogenic stage of the anaerobic fermentation, it is necessary to break the complex structure of RS to liberate the soluble sugar monomers. This difficulty in the solubilisation of RS is because the fermentable polysaccharide sugars (hexose and pentose) are masked by a non-fermentable lignin polymer [18,28,29,50,51]. Similarly, lignocellulose can resist degradation due to its cell walls, which gives them hydrolytic stability and structural robustness [48]. The structural strength comes from the cross-linking of polysaccharide sugars (cellulose and hemicellulose) with complex aromatic polymer (lignin) through ester and ether linkages [51]. Hence, for effective hydrolysis, it is pertinent to separate cellulose from the lignin and rearrange the ultrastructural components to increase the surface area to a final particle size of 0.2–2 mm [48]. This deconstruction of the RS structure is achieved through various levels of PTMs.

In the study, PTM of RS was performed using 1 M HCl and 2% NaOH. In addition, PE, as defined in Section 2.4, was employed in the PTM. The delignification measurement illustrated in Fig. 2 indicated the rate of lignin dissolution during PTMs of different RS substrates. The SEM micrographs of RS for untreated RS, HCl, NaOH and PE-PT RS are also shown in Fig. 3.

The SEM results showed noticeable morphological and histological changes, more evident in NaOH and PE-PT RS residues. Similarly, the pictorial representation of the different PT RS residues is shown in Fig. 4. As shown from the figure; there were morphological and physical changes that were brought about by physical and chemical PTMs as seen from "A and B" corresponding to 2 mm sized RS and 750 μm RS powder and from "C to E" analogous to different chemical PT RS residues (NaOH, HCl, PE-PT RS). The physical configuration of RS is the same as that obtained by Zhang and Cai [105], who recorded structural changes in their work on enzymatic hydrolysis of alkali PT RS by *Trichoderma reesei* ZM4-F3. Similar structural changes were achieved by Cai et al. [18].

Morphologically, NaOH-PT RS had a woolly and curled appearance after PTM. In contrast, PE-PT RS was wholly and had improved the particles' individuality after PTM (Fig. 4). The histological alterations in these residues were a result of the cleavage of lignin ester and ether bonds [18,87], which created micro-pores and made the RS structure shrink giving rise to significant histological changes (Fig. 3) [25]. The result was also in tandem with the findings from the delignification analysis (Fig. 2), where it was observed that lignin loss from NaOH and PE-PT RS residues were more (25 and 17%, respectively) compared to the control. The lignin removal is consistent with the result of Zhao et al. [108], with lignin loss within the 7–17% range. Therefore, the delignification from NaOH and PE-PT RS residues could be from the dissolution of lignin components, leading to the rupturing of intermolecular bonds between lignin and hemicellulose [25,60,89]. Thus, this lignin solubilisation improved the porosity of the RS biomass [87] and the yield of cellulose. In addition, lignin dissolution is probably from the anionic and earth elements in PE (Table 1) and NaOH. In Eastern Nigeria, PE is added as a softener when cooking hard and dry seeds or meats. This supplementation quickens the tenderness or shortens the time spent in meal preparation.

The structural changes of the HCl-PT RS samples resulted from hydrolysis of both the cellulose and hemicellulose through the breakdown of the β, 1–4 glucosidic bonds and the reduction of the OH groups of the glucosidic bonds [46,87]. This disruption made the fibrils collapse and look sparse. Therefore, more levels of reducing sugar in the HCl-PT supernatant. In contrast, the raw RS (control) sample showed rigid and highly organised fibrils after grinding (Figs. 3 and 4). These results agreed with the outcomes of Cheng et al. [25] on microwave-assisted
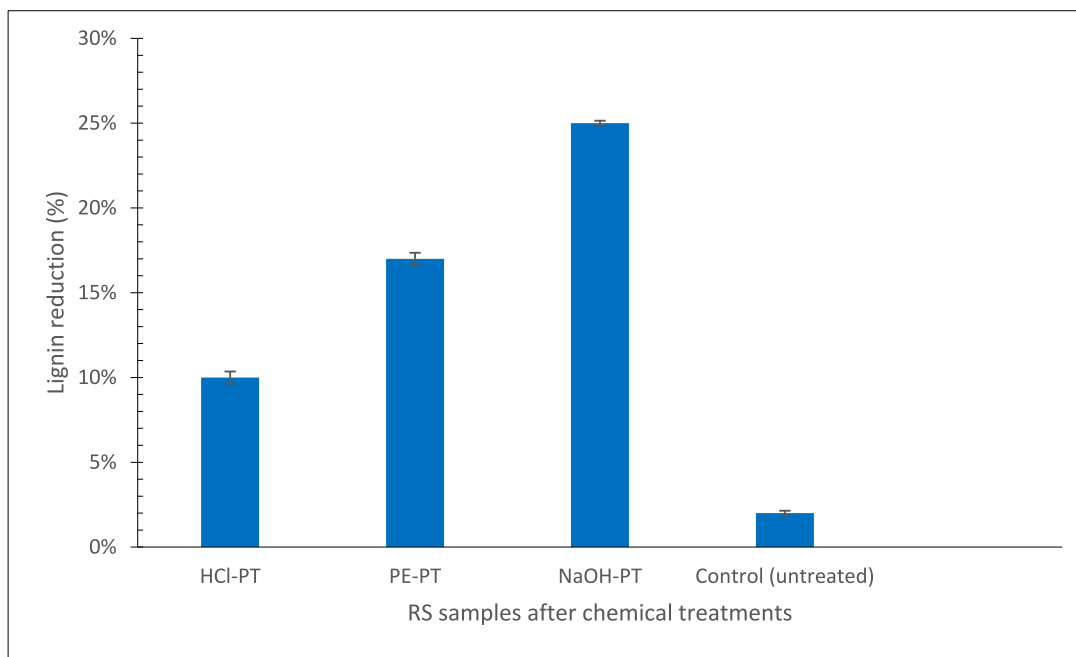
Fig. 2. Delignification of some chemical and PE-PT RS samples represented as percentage lignin loss.

alkali PTM of RS and Pan et al. [77] on dilute acid hydrolysis on cornstalks.

3.1.2. Characterisation of chemically-PT RS hydrolysates

The RS filtrates, after various PTMs, were analysed for reducing sugar concentration (RSC), chemical oxygen demand (COD), and total carbon content (TCC) (Table 7). The RSC (g L^{-1}) and the TCC (mg L^{-1}) of the filtered (detoxified) RS hydrolysates were lower than the unfiltered RS hydrolysates. The weight difference could be from some RS PTMs inhibitors removed during filtration.

These inhibitors, which may inhibit fermentation processes, are furan derivatives, such as furaldehyde (furfural) and 5 – hydrox-ymethylfurfural, phenolic compounds (vanillin and syringaldehyde) and salt complexes [30,46,64]. These contaminants affect glycolysis, damage cell membrane and DNA and cause a total shift in the fermentation pathway [16,30,46]. Therefore, it could be said that the lime–treatment and pH neutralisation before filtration perhaps removed some of these inhibitors ([76,88]. Nevertheless, removing inhibitors decreases the filtrate's total organic content (RSC).

The RSC of 6.64 g L^{-1} and the total organic carbon (TOC) of 11.52 g L^{-1} of PE-PT RS filtrate were slightly closer to that of HCl-PT RS filtrates with RSC of 7.28 g L^{-1} and the TOC of 11.32 g L^{-1}; and NaOH-PT RS filtrates with RSC of 6.88 g L^{-1} and the TOC of 13.48 g L^{-1} (Table 7). In contrast, the control had the lowest RSC of 0.88 g L^{-1} and TOC of 2.16 g L^{-1}. These values differ significantly from those of Chang et al. [22] on RS hydrolysis. They reported that about 99.3 g L^{-1} of hexose and 80.1 g L^{-1} of pentose could be obtained from 30 g of RS in 100 mL water. However, in RS hydrolysis by Kim et al. [46], an RSC of 16.8 g L^{-1} was achieved using 0.5% H$_2$SO$_4$ and <1.0 g of RSC employing an alkali (NaOH). The different PTM methods, PTM agents, and hydrolysis conditions such as temperature, duration of PTM and RS ratio volume could explain the reason behind the variation in sugar yield.

3.1.3. Enzymatic hydrolysis of chemically-PT RS residues

The dried HCl, NaOH, and PE-PT RS samples and raw RS were enzymatically hydrolysed with cellulase (0.8 U mg^{-1}). However, before applying to different RS samples, the optimal hydrolysis conditions in terms of concentration of the cellulase enzyme (0.2 to 2.0 g) per 1 g RS sample and hydrolysis time (0 to 5 d) were established following the

method outlined in Section 2.6 and using NaOH-PT RS as feedstock. The cellulase activity at various concentrations and durations is represented in Fig. 5. From the figure, although there was a consistent increase in RSC and TOC at all different levels of cellulase employed from the first day, there were no significant changes in RSC and TOC as cellulase concentration was increased to 1 and 2 g from day 2 to 5. In contrast, RSC and TOC levels increased from 24 to 48 h when the enzyme concentration of 500 mg was used. The RCS and TOC also grew linearly until "day 5", when the enzyme at 200 mg amount was employed. The RSC and TOC levels were inconsequential in the control samples without cellulase.

Hence, the cellulase concentration at 500 mg and the duration of 48 h were established and employed as the ideal concentration and time for the enzyme hydrolysis of the different residual PT RS. Even though the selected optimal conditions obtained vary from the results obtained by Zhang and Cai [105] and Cai et al. [18], the result obtained is in line with the method employed by Pan et al. [77] on bio-augmented cellulosic hydrogen production from cornstalk. Furthermore, the established optimal standards tally closely with the findings by Gao et al. [33] in their work on enhanced enzymatic hydrolysis of RS via PT with deep eutectic solvent-based micro-emulsions. The established duration of 48 h employed in the hydrolysis was also within the range of 24–50 h used by Quéméneur et al. [83]. The disparities from the outcome of Zhang and Cai's [105] and Cai et al. [18] studies could be from RS sample sizes, the nature and purity of the enzyme materials and the mode of enzymatic hydrolysis.

After the ideal conditions were determined, the enzymatic hydrolysis of the various PT RS residues and untreated (raw) RS was carried out. Subsequently, after the enzyme solubilisation, the pH of the different PT RS hydrolysates was 6.0 ± 0.5. The experimental result of the RSC, TOC and enzymatic conversion rate from the various PT RS feedstocks is summarised in Table 8. From the table, NaOH and PE-PT RS residues had the highest enzyme conversion rate of 36 and 28%, respectively. Therefore, the reducing sugar (0.49 0.62 g gTS^{-1} RS) yield of the various RS PT residues is almost close to the maximum predicted value of 0.56 obtained by Pan et al. [77], even though the substrates employed are different. The RSC were also within the range of 0.39 and 0.74 g g^{-1} RS achieved by Cai et al. [18] for RS PTMs. Cheng et al. [25] obtained a similar result of 0.69 g g^{-1} RS as the maximum RSC from PT RS.
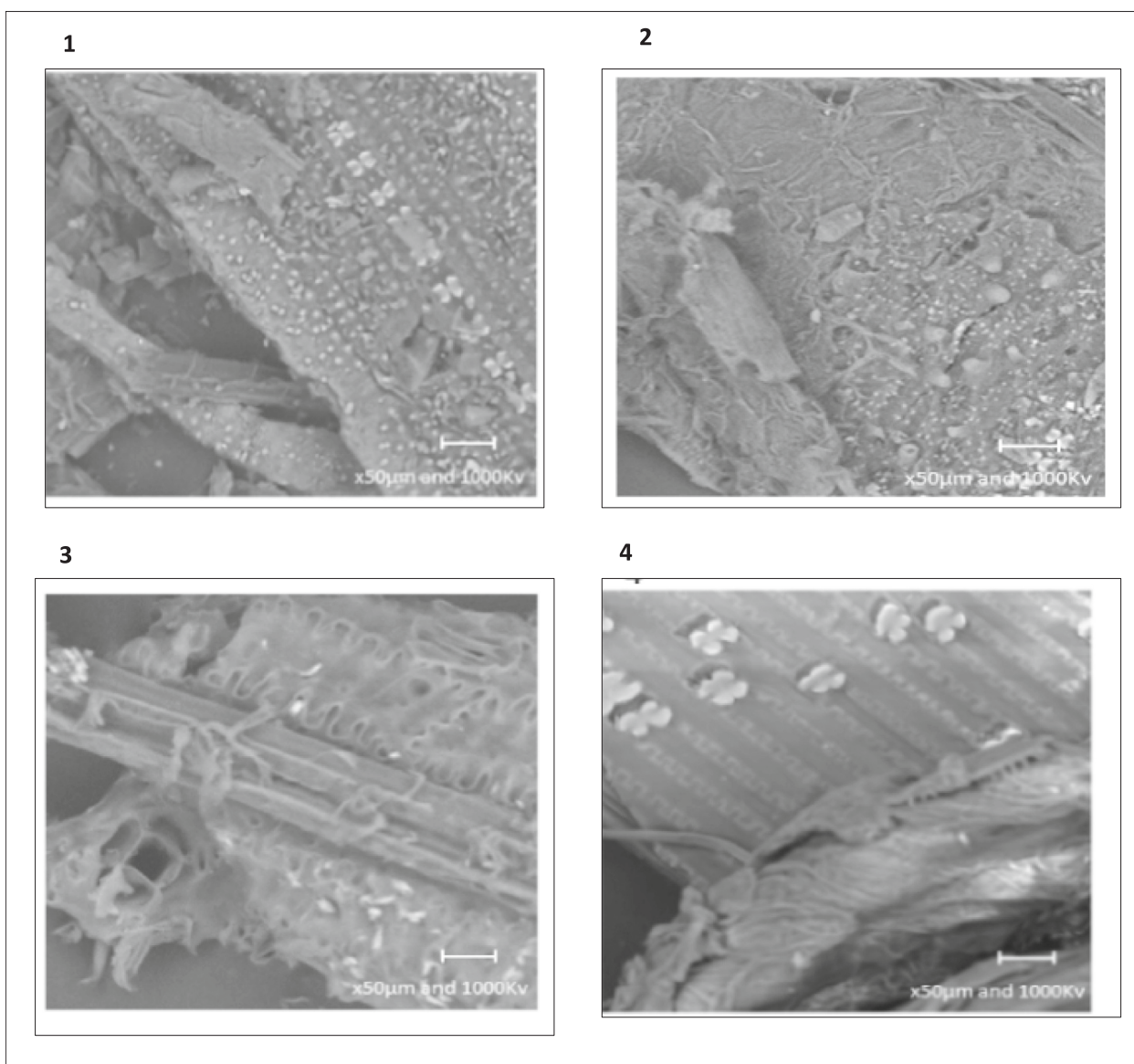
Fig. 3. SEM micrographs of raw RS (1) and various PT RS (2: HCl, 3: PE and 4: NaOH) samples.

In addition, the highest RSC (34.0 and 30.5 g L^{-1}) and TOC (37.3 and 33.4 g L^{-1}) from NaOH-PT RS and PE-PT RS, respectively, show that the cellulase enzyme had more access to the RS hollo-cellulose components. The enzyme accessibility is a result of the removal of lignin (Fig. 2) and the creation of micro-pores on the RS structure following PTM [87,105] with either NaOH or PE when compared with raw RS which had the least enzyme conversion rate of 8% with resultant 8.5 g L^{-1} of RSC and TOC of 10.5 g L^{-1}. Although the enzyme conversion rate from HCl PT RS residue was 17%, the reducing sugar (26.5 g L^{-1}) and TOC (30.2 g L^{-1}) (Table 8) were found to be nearly as close as to those of NaOH and PE despite having reduced delignification activity (Fig. 2). The good yield of sugars could be from the exposure of cellulase enzyme to cellulose brought about by the rupturing of β 1, 4-glucosidic bonds and hence, some collapse of the cellulose polymers to sugars monomers. The result was also confirmed from the SEM images reported above (Fig. 3). A small amount of VFA, mainly acetic acid in all the PT samples, could not be explained (Table 8). Nonetheless, it is suggested they could have emanated from the gradual degradation of reducing sugars during post-hydrolysis processes and possibly during storage before application for hydrogen production.

3.2. Hydrogen fermentation process (stage 1 process)

The hydrogen yield from chemically-PT RS hydrolysates ranged from 10 to 15 NmL H$_2$ g^{-1} COD (data not included), which is a result of low RSC (Table 8) and the presence of inhibitors [46,50,64,84]. This idea asserts the results obtained by Chang et al. [22] and reviews by Kapdan and Kargi [44] on their assessment of bio-H$_2$ production from wastes, where it was shown that H$_2$ could be produced in high quantities from assimilable sugar-containing wastes under specified conditions. In addition, hydrogen is generated as a *by-product* of glucose consumption during the acidogenic phase in an AD process. Therefore, the yield of hydrogen gas correlates directly with the amount of glucose in a solution or substrates [65], while the evolution of H$_2$ responds inversely to RSC decreases. These arguments are affirmed by the yield of H$_2$ from enzymatically-PT RS hydrolysates (Fig. 6 and Fig. 7).

After the enzyme hydrolysis of the various PT RS residues, the resultant hydrolysates containing reducing sugar were pooled together and transformed into H$_2$ and biogas using a batch and continuous process. The daily specific hydrogen production (SHP) and hydrogen content of enzymatically-PT RS hydrolysates are shown in Fig. 6 and Fig. 7. It is observed from the batch result that while the specific biogas yield
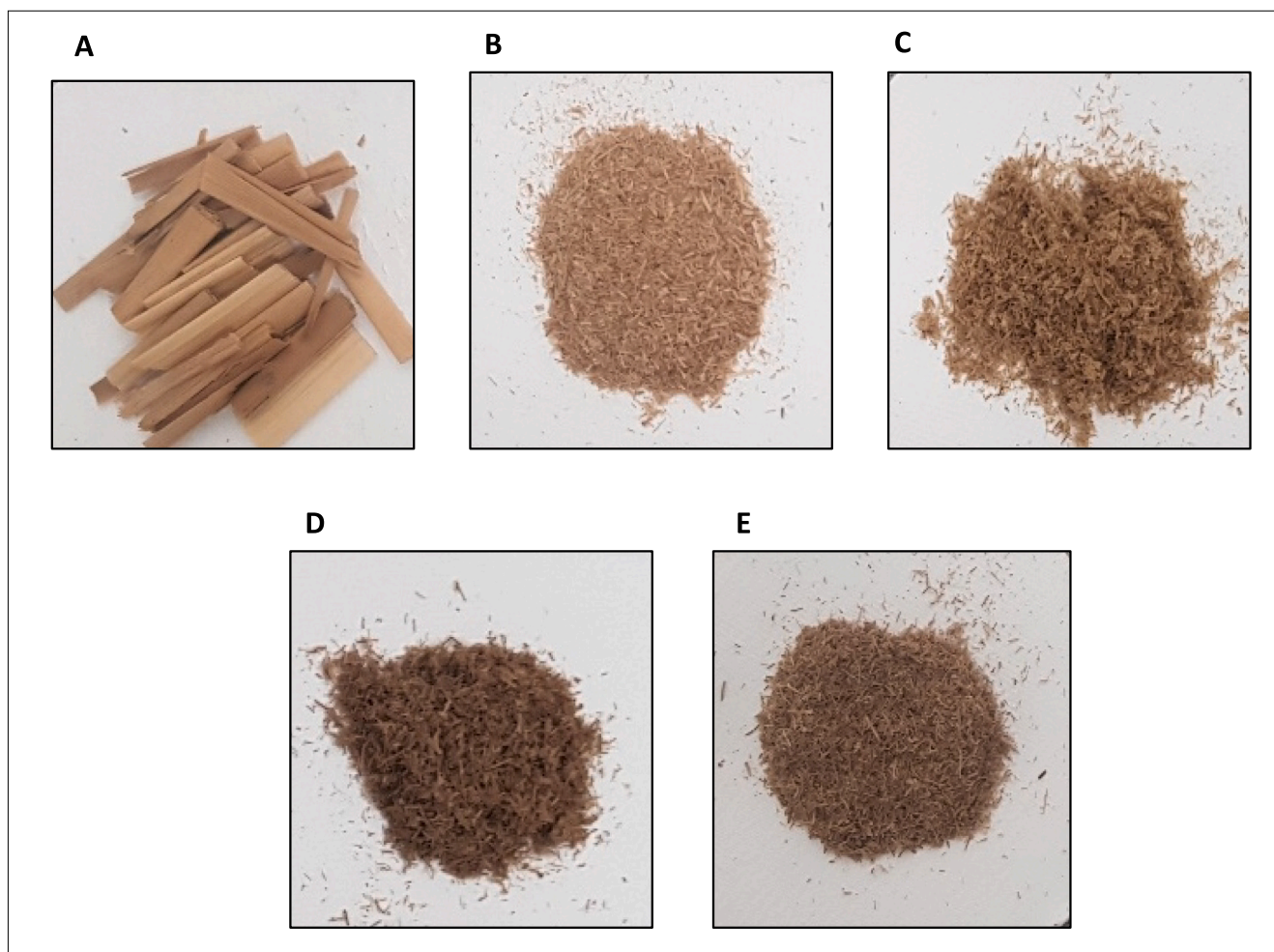
Fig. 4. PT RS samples (A: 2 mm sized RS; B: Milled RS; C: NaOH-PT RS; D: HCl-PT RS; E: PE-PT RS).

Table 7
Characterisation of raw and various PT RS filtrates.

RS filtrates	Reducing sugar (g L^{-1})	COD (g L^{-1})	Total carbon (g L^{-1})	Inorganic carbon (g L^{-1})	Total organic carbon (g L^{-1})
HCl-PT	7.28	19.90	11.32	0	11.32
HCl-PT filtered	4.52	7.50	5.26	0	5.26
NaOH-PT	6.88	16.50	13.48	0.23	13.25
NaOH-PT filtered	4.36	10.10	6.30	0	6.30
PE-PT	6.64	17.00	11.52	1.39	10.14
PE-PT filtered	4.40	8.10	6.64	0	6.64
Control (untreated)	0.88	4.70	2.16	0	2.16
Control filtered	0.54	2.90	1.47	0	1.47

(SBY) was 321 NmL g^{-1} sugar-utilised, the specific hydrogen yield (SHY) and the mean hydrogen content were 221 NmL H$_2$ g^{-1} sugar-utilised and 55%, respectively (Fig. 6). The hydrogen content was close to 60.9% attained by Kim et al. [47]. Furthermore, the maximum hydrogen rate was 104 ± 2 NmL H$_2$ d^{-1}. The hydrogen production profile was simulated by a modified Gompertz equation, and the R-square value of 0.999 showed that the fermentation process was good. However, the production rate disagrees with those obtained by Lo et al. [60] using xylanase on alkaline-PT RS and Kannah et al. [43] bio-hydrogen production from

RS PT with dispersion thermochemical disintegration. The disparities could be due to differences in the type and concentration of enzyme utilised, mode of alkaline PTM and enzyme hydrolysis, and duration of H$_2$ production.

Nonetheless, the hydrogen yield tallies with Dong et al. [29] findings, where the maximum H$_2$ produced is 213.06 NmL H$_2$ g^{-1} substrate after PTM of RS with 3% NaOH and 6% urea for 15 days. The study also agrees closely with those obtained by Cheng et al. *[25]* on H$_2$ production from PT RS. They achieved a maximum hydrogen yield of 155 NmL H$_2$ g^{-1} TVS after RS was PT with microwave-assisted alkali in addition to enzymatic hydrolysis. The research findings are consistent with An et al. [8] and Zhang et al. [106]. They produced a SHY of 226 NmL g^{-1} substrate and 222 NmL H$_2$ g^{-1} sugar-utilised.

Similarly, the result of CSABR indicated that the hydrogen content was within the range of 53–56%, and the minimum and maximum daily SHP of 163 and 185 NmL H$_2$ g^{-1} sugar-utilised. d^{-1} respectively were achieved (Fig. 7). The mean SBY from the CSABR fermentation was 321 NmL g^{-1} COD sugar-utilised d^{-1}. The result obtained from the batch and continuous systems was validated using the theoretical yield of hydrogen from RS and was within the range. The theoretical hydrogen yield from RS using an AD system is 301 NmL H$_2$ g^{-1} TVS [25]. Although the maximum SHY of 209.8 mL g^{-1} TVS achieved by Pan et al. [77] is slightly higher than the obtained values from this study via CSABR, the key differences perhaps are from the feedstock and processes applied. In the batch and CSABR hydrogen fermentation systems, the mixed H$_2$ gas was methane free.

The specific hydrogen and biogas yield using hydrolysates from
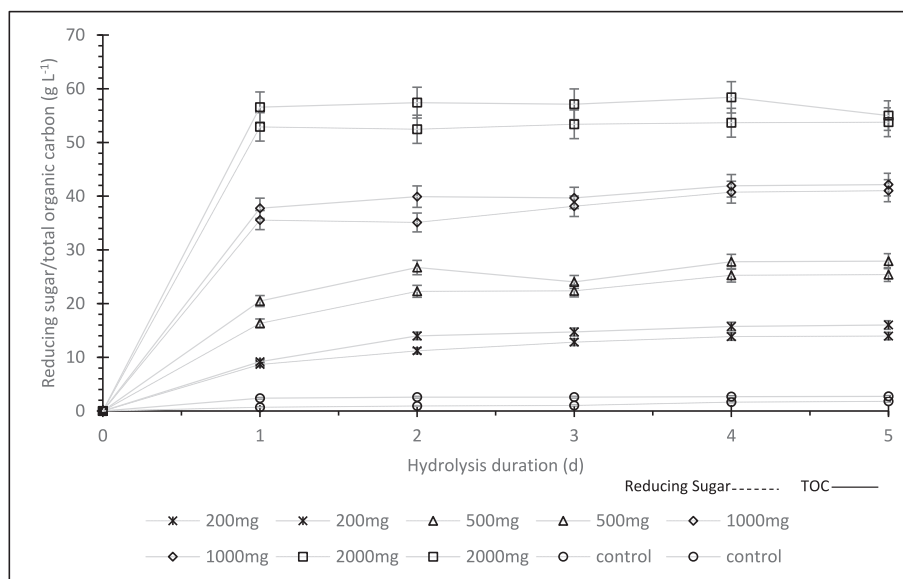
Fig. 5. Cellulase activity at various concentrations and durations.

Table 8
Analysis of enzymatically-PTRS Hydrolysates.

RS residues	Enzyme conversion (%)	Reducing sugar (g L^{-1})	Reducing sugar (g gTS^{-1} RS)	TOC (g L^{-1})	TVFA (g L^{-1})
HCl-PT	17	26.5	0.49	30.2	0.02
PE-PT	28	30.5	0.56	33.4	0.03
NaOH-PT	36	34.0	0.62	37.3	0.04
Raw (untreated)	8	8.5	0.16	10.5	0.012

various PT RS residues are presented in Table 9 for batch and continuous systems. The cumulative and daily biogas production was almost in the same range for the reactor systems. NaOH and PE-PT RS hydrolysate had the highest values of 199 and 179 NmL g^{-1} TS RS, respectively, when the continuous system was used. The SBY for HCl-PT RS and raw RS hydrolysate from Table 8 was 159 and 51 NmL g^{-1} TS RS under CSABR mode. While the SHY from batch and the daily SHP from CSABR systems differed slightly, the highest values were from NaOH-PT hydrolysates (batch (137 NmL H$_2$ g^{-1} TS RS d^{-1}) and CSABR (114 NmL H$_2$ g^{-1} TS RS d^{-1})) and PE-PT RS filtrates (batch (123 NmL H$_2$ g^{-1} TS RS d^{-1}) and CSABR (103 NmL H$_2$ g^{-1} TS RS d^{-1})).

In contrast, raw (untreated) RS hydrolysate gave cumulative H$_2$ production of 35 NmL H$_2$ g^{-1} TS RS d^{-1} from batch mode and SHP of 30 NmL H$_2$ g^{-1} TS RS d^{-1} from continuous mode (Table 9). Subsequently, the SHP of HCl-PT RS samples was 109 NmL H$_2$ g^{-1} TS RS d^{-1} from the batch systems and the SHP of 91 NmL H$_2$ g^{-1} TS RS d^{-1} from CSABR. These results show that chemical PTM before enzymatic exposure of lignocellulose is essential to ensure maximum hydrolysis and increased evolution of H$_2$. RS pretreatment enhances lignocellulose properties for improved enzyme accessibility and AD process efficiency, as seen from the SEM micrograph (Fig. 3). The SHY values are slightly close to the
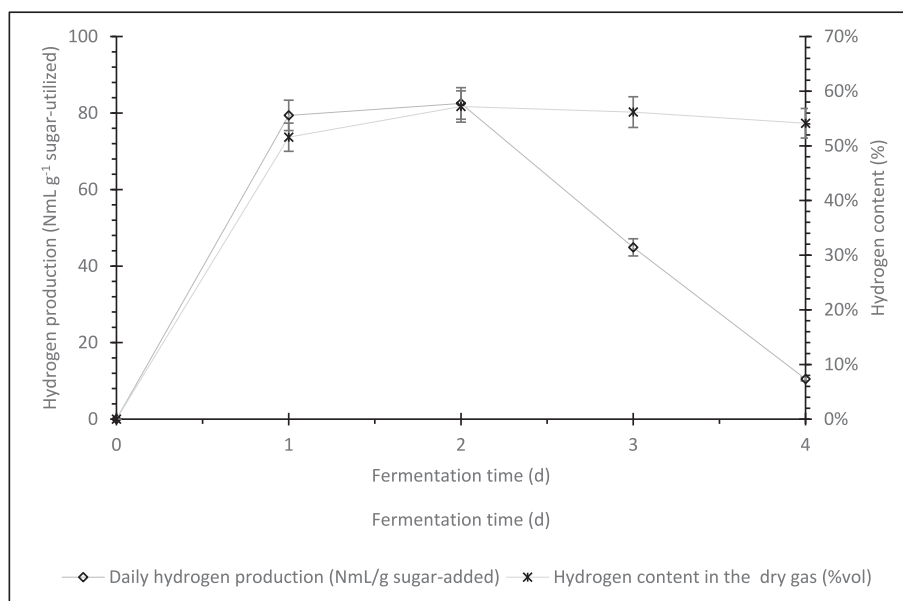
Fig. 6. Daily hydrogen production and hydrogen content from enzymatically-PT RS residues via batch mode.
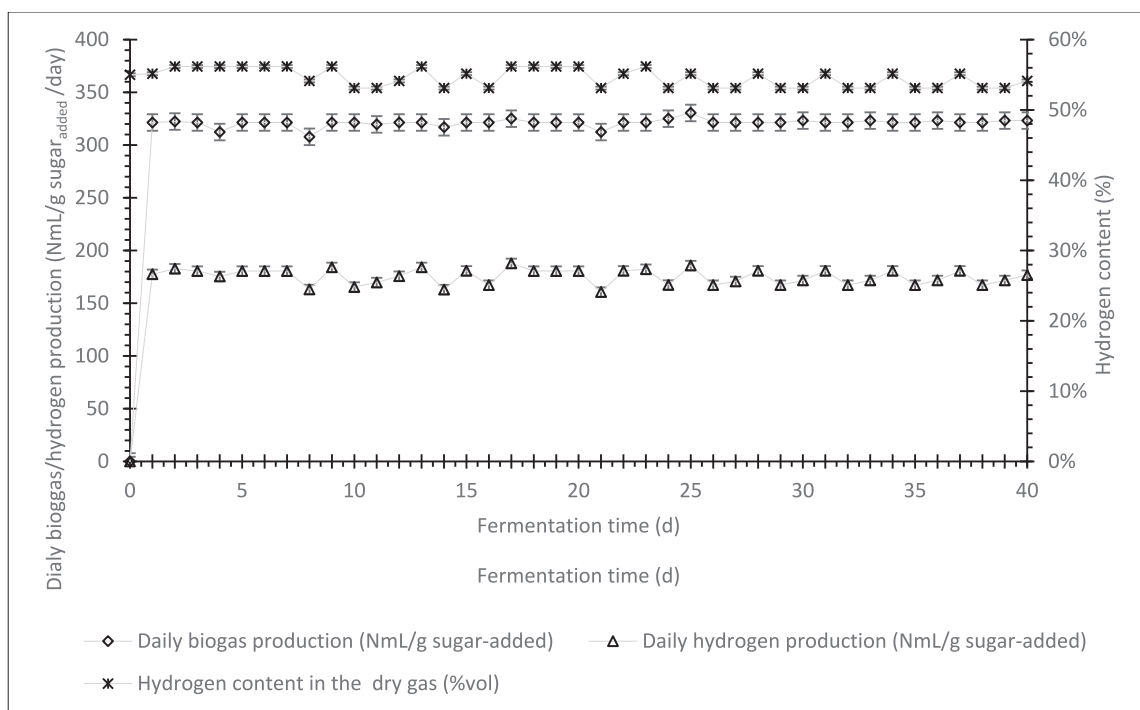
Fig. 7. Daily hydrogen production and hydrogen content from enzymatically-PT RS residues via CSABR.

Table 9
Hydrogen and biogas yield using hydrolysates from various PT RS residues.

RS hydrolysates	Reducing sugars (g gTS^{-1} RS)	Batch reactor		Continuous reactor	
		Cumulative H$_2$ production (NmL g^{-1} TS RS)	Cumulative biogas production (NmL g^{-1} TS RS)	Daily H$_2$ production (NmL g^{-1} TS d^{-1})	Daily biogas production (NmL g^{-1} TS d^{-1})
HCl-PT	0.49	109	159	91	159
PE-PT	0.56	123	179	103	179
NaOH-PT	0.62	137	198	114	199
Raw (untreated)	0.16	35	51	30	51

Note: Result values were calculated from the data obtained from Figs. 6 and 7, and Table 8 with delignification percentage (Fig. 2) was also considered.

hydrogen production performance of 125 and 163 NmL H$_2$ g^{-1} TS RS for NaOH/Urea and electro-hydrolysis PTMs respectively attained by Cai et al. [18] via the batch system. Cheng et al. [25] achieved SHY of 108–155 NmL H$_2$ g^{-1} TS RS in microwave-assisted alkali pretreatment of RS to promote enzymatic hydrolysis, which slightly agrees with the laboratory SHY values. Although the SHY 168 NmL H$_2$ g^{-1} TS obtained by Zhang et al.[107] on bioH$_2$ production from cornstalk hydrolysate is slightly higher than the study SHY, the differences could be from the type of substrate and conditions of pretreatment employed.

$$C_6H_{12}O_6 + 2H_2O \rightarrow \underset{Acetic\ acid}{CH_3COOH} + 2CO_2 + 4H_2 \qquad (10)$$

$$C_6H_{12}O_6 \rightarrow \underset{Butyric\ acid}{CH_3CH_2CH_2COOH} + 2CO_2 + 2H_2 \qquad (11)$$
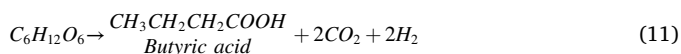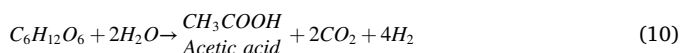
3.3. Distribution of short-chain fatty acids from acidogenic reactors

The low levels of SCFA in the hydrolysates after enzymatic PTM (Table 8) did not inhibit H$_2$ fermentation due to the high content of reducing sugars in the various hydrolysates that favours acidogenesis. Hence, the H$_2$ and CO evolution with more volatile fatty acids. The most predominant SCFA after the batch fermentation, which was acetic acid (HAc) (360.80 mg L^{-1}), butyric acid (HBu) (792.8 mg L^{-1}) and formic acid (HFo) (78.9 mg L^{-1}), agrees with the report of Ai et al. [4], Kim et al. [47] and Li et al. [56]. Fig. 8 shows the associated TVFA production

after H$_2$ fermentation for continuous systems. The pH after batch fermentation which was found to be 4.85 ± 0.5 (Table 10), indicated the production of VFA during H$_2$ fermentation (Eqs. 10 and 11). As such, the pH of the continuous system was maintained at 5.5 ± 0.2 using 5 M NaOH. The production of various SCFAs also affirmed the hydrogen production rate from batch and continuous systems (Figs. 6 and 7). Butyrate was produced more than HAc and HFo, indicating that the fermentation pathway was mainly from the pyruvate: ferredoxin oxidoreductase (PFOR) [39,69]. There was an insignificant propionic acid concentration (200 ɳg L^{-1}), signifying less solvent production tendencies. After the steady state was established, the mean daily TVFA was 1232.5 mg L^{-1}, comprising acetic acid, butyric acid, and formic acid as 355.4 mg L-1, 787.8 mg L-1 89.3 mg L^{-1}, respectively (Fig. 8). Similarly, daily soluble COD (SCOD) of the CSABR effluents were within the range of 1415.30 to 1435.60 mg L^{-1}.

$$CH_3COOH \rightarrow CH_4 + CO_2 \qquad (12)$$

$$\underset{Propanoic\ acid}{4CH_3CH_2COOH} + 2H_2O \rightarrow 7CH_4 + 5CO_2 \qquad (13)$$
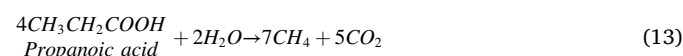
3.4. Production of methane from acidogenic effluents (stage 2 process)

In the fermentative hydrogen production from glucose, as previously stated, there is concomitant evolution of SCFA with acetate (Eq. 10) and butyrate (Eq. 11) as the most important soluble metabolites (Fig. 8 and
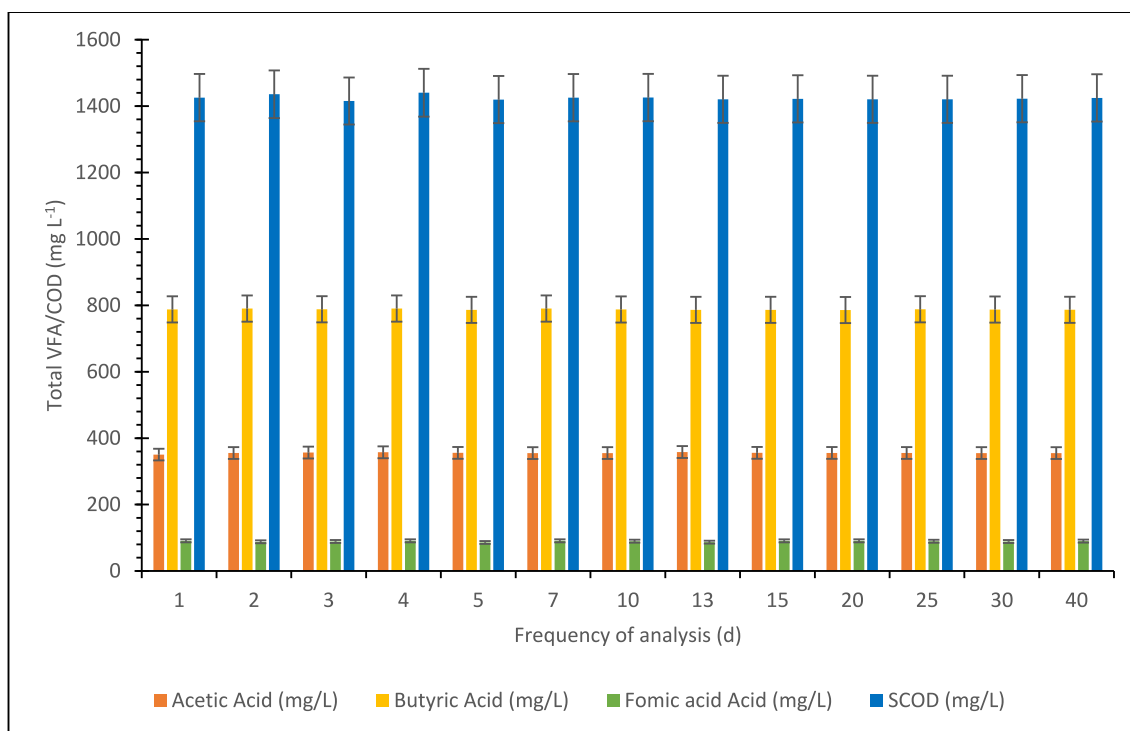
Fig. 8. The TVFA production after H_2 fermentation from continuous systems.

Table 10
VFA, SCOD and nitrogen content of reactor effluents and methane sludge.

Sample source	Acetic acid (mg L^{-1})	Butyric acid (mg L^{-1})	Formic acid (mg L^{-1})	Soluble COD (mg L^{-1})	pH value	Ammonium nitrogen (mg L^{-1})
Heat-shocked DCS	407.25	270.00	107.80	920.45	8.62 ± 0.4	272.00
H_2 batch reactor	587.81	607.34	186.70	1640.43	4.85 ± 0.5	263.50
Initial H_2 CSABR	280.56	235.60	89.34	970.80	4.87 ± 0.3	230.52
ADS	780.24	220.78	NA	1210.65	8.50 ± 0.3	263.76
CH_4 digesters	~400.00	~121.00	NA	~600.00	6.89 ± 0.3	~225.00
VFA-CH_4 batch digesters	25–30	NA	NA	NA	7.03 ± 0.2	NA.

Table 10). These organic acids (including propanoic acid) were utilised in methane gas production (Eqs. 12 and 13) to maximise the overall economic and energy value of the RS biomass. The fermentation was done using a fed-batch process before switching the reactor to continuous mode via the CSABR system. Once the steady state is established in the stage 2 process, the effluents from acidogenic continuous reactors were fed directly to the CSABR for methane production after debris removal.

The methane production using acidogenic effluent as substrate via the fed-batch system is presented in Fig. 9. It can be observed from the graph that methane was produced spontaneously within the first 4 d, which shows that acidogenic effluent is an ideal substrate for methane production [9,47,82]. Furthermore, the acclimatisation of ADS with SCFA was also the reason for the high methanogenesis rate. Most methanogens, especially the acetoclastic methanogens, grow slowly (*Methanosaeta* generation time is 3.4–9.0 d), which is attributed to the low energy yield of the methanogenesis pathway [35]. However, the acclimatisation period ensures the complete growth of most acetoclastic methanogens.

The mean specific methane yield (SMY) of 362 NmL CH_4 g^{-1} COD$_{consumed}$ and the mean biogas yield of 465 NmL g^{-1} COD$_{consumed}$ were produced using the fed-batch systems after 3 HRTS (Fig. 9). The reactors' highest and mean methane content of 80 and 75% were achieved using the fed-batch approach. Subsequently, the result of the continuous methane production from acidogenesis effluents is shown in Fig. 10. The

result obtained showed that the mean daily specific methane production (SMP) was 330 NmL CH_4 g^{-1} COD$_{consumed}$ d^{-1}, and daily biogas yield was 411 NmL g^{-1} COD$_{consumed}$ d^{-1}, while the average methane content is 80%.

The theoretical methane yield at standard temperature and pressure for 1.0 g CH_3COOH and 1.0 g CH_3CH_2COOH is about 400 and 570 mL, respectively [108]; therefore, the findings are within the range of theoretical values. The results achieved were close to the study outcome by Akobi et al. [6] and An et al. [8,9]. Methane production of 369, 341 and 376 NmL g^{-1} COD$_{consumed}$, respectively, were recorded from first-stage acidogenic effluents. The consumption of TVFA to methane was confirmed following an analytical test before and after batch fermentation, where the remaining VFA contents from the methane reactors were almost negligible (HAc 25–30 ± 0.2 mg L^{-1} (Table 10). The COD removal/ conversion rate of 81% for methane production at steady-state and 91% at batch system tallies with Kim et al. [47] and Akobi et al. [6] study. The conversion rate was calculated by dividing the methane accumulation by the theoretical methane yield of 400 mL g^{-1} COD$_{consumed}$ at 37 °C [9].

The specific methane and biogas yield using acidogenic effluents from various PT RS residues is presented in Table 11 for batch and continuous systems. The table was calculated using Eq. 1, and the SCFA produced daily, which was 615 mg L^{-1} g^{-1} sugar-utilised. The daily SCFA value was obtained from the difference between the daily TVFA (Fig. 8) and the initial TVFA from the DCS (Table 10). The SMY and
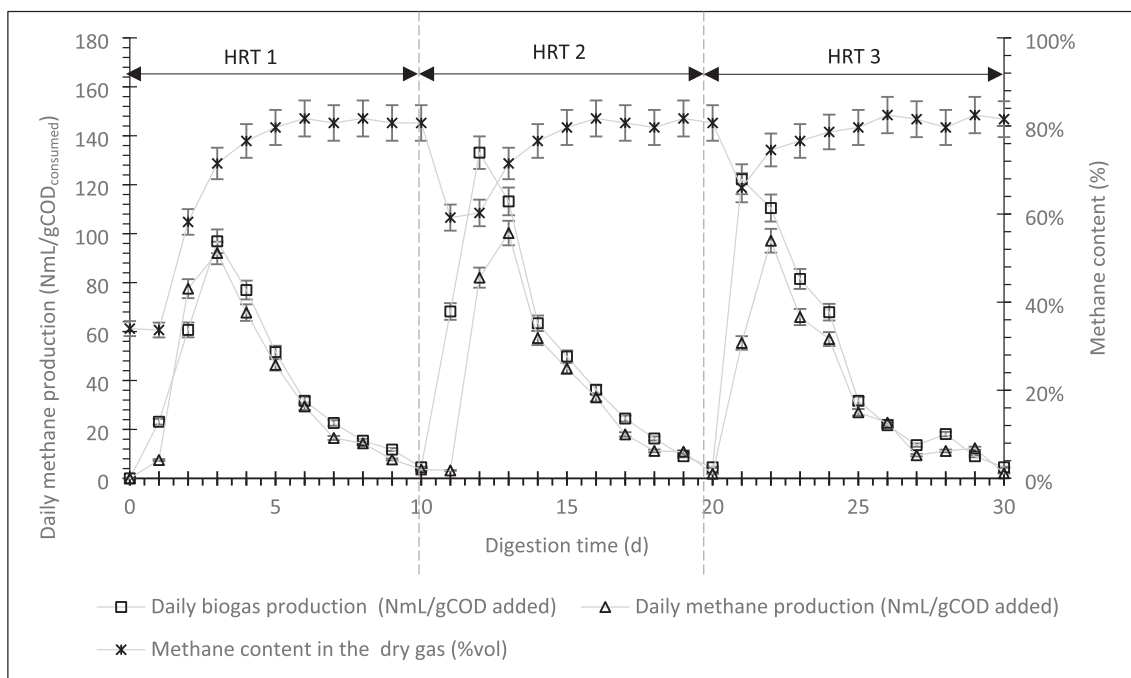
Fig. 9. Methane production using SCFA as feedstock via the fed-batch mode after 3 HRTs.
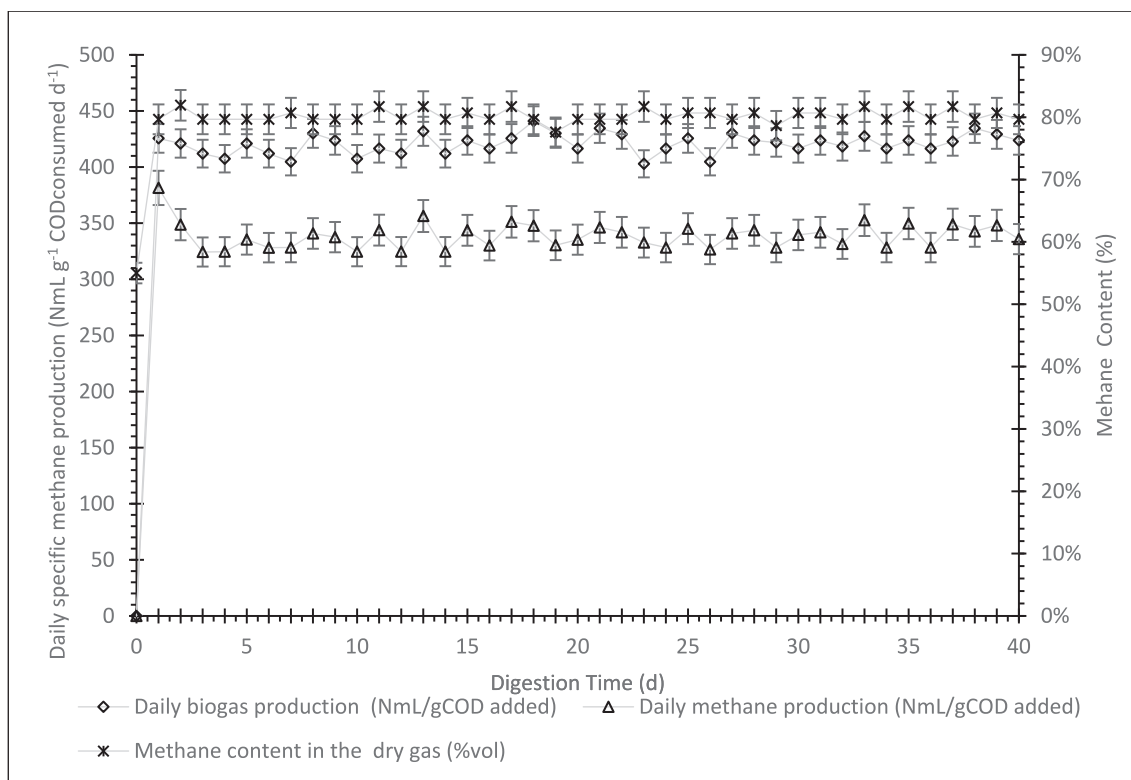
Fig. 10. Continuous methane production employing acidogenesis effluent as feedstock.

biogas accumulation was significantly higher from PT RS residues than the untreated RS for the two systems, with NaOH and PE-PT RS hydrolysate showing the highest values (Table 11). In the batch mode, NaOH PT reactors gave 138 NmL CH_4 g^{-1} TS and 177 NmL g^{-1} TS for SMY and biogas yield, whereas PE-PT reactors had 124 NmL CH_4 g^{-1} TS and 159 NmL g^{-1} TS for SMY and biogas yield. A similar outcome was achieved for continuous systems where NaOH PT reactors gave 126 NmL

CH_4 g^{-1} TS and 156 NmL g^{-1} TS for daily SMP and biogas production, respectively (Table 11). PE-PT reactors also had 113 NmL CH_4 g^{-1} TS and 141 NmL g^{-1} TS for daily SMP and biogas production. The increase in SMP, SMY, daily biogas production, and biogas yield from PT RS samples is because of improved production of TVFA during their respective acidogenesis in stage 1 of 0.30 to 0.38 $gCOD^{-1}$ gTS compared to raw RS that gave TVFA of 0.10 $gCOD^{-1}$ gTS (Table 11).

Table 11

CH$_4$ and biogas yield using acidogenic effluents from various PT RS residues.

RS hydrolysates	TVFA (gCOD^{-1} gTS)	Batch reactor		Continuous reactor	
		SMY (NmL g^{-1} TS)	Biogas yield (NmL g^{-1} TS)	Daily SMP (NmL g^{-1} TS d^{-1})	Daily biogas (NmL g^{-1} TS d^{-1})
HCl-PT	0.30	110	142	100	125
PE-PT	0.34	124	159	113	141
NaOH-PT	0.38	138	177	126	156
Raw (untreated)	0.10	36	46	33	41

The table above is calculated from acidogenic effluents with 1.0 g reducing-sugar producing 615 mg L^{-1} TVFA (comprising of HAc (175.4 mg L^{-1}), HBu (317.5 mg L^{-1}) and HFo (89.3 mg L^{-1})) and from Table 8.

3.5. Production of methane from enzymatically-PT RS residues (stage 3 process)

The leftover residues from the various enzymatically-PT RS were employed for methane production via batch and continuous systems. Nevertheless, the control (raw/untreated RS) was also used for practical comparison analysis, as described in Section 2.8.2. Fig. 11 (a-d) shows the methane production from different PT RS residues using batch mode, while Table 12 is the revised Gompertz data for the batch methane production from the various PT RS residues. The highest SMY of 360 NmL CH$_4$ g^{-1} TS and 335 NmL CH$_4$ g^{-1} TS with volumetric methane production rates of 38.07 mL d^{-1} and 33.85 mL d^{-1} were obtained from NaOH and PE-PT RS residues, respectively, compared to SMY of 267 NmL CH$_4$ g^{-1} TS with a methane production rate of 22.22 mL^{-1} d from raw RS (control). In addition, the SMY of 303 NmL CH$_4$ g^{-1} TS with a methane production rate of 23.17 mL d^{-1} was recorded from the HCl-PT RS sample. The result is consistent with the values of Mustafa et al. [68] on fungal PTM of RS with *Pleurotus ostreatus* and *Trichoderma reesei* to enhance methane production under solid-state anaerobic digestion. Similarly, the result is within the values obtained by Kainthola et al. *[42]* on enhanced methane potential of RS with microwave-assisted PTM. They reported methane production of 325 NmL CH$_4$ g^{-1} VS for microwave PT RS, while untreated RS was 231 NmL CH$_4$ g^{-1} VS. Moreover, the SMY from the raw RS is within the values obtained by Lei et al. [54]. Nevertheless, the result differs from those of Zhao et al. [108] on methane production from RS pretreated by a mixture of acetic-propionic acid. They reported that the final output of 280 NmL CH$_4$ g^{-1} VS d^{-1} was obtained from PT RS, while the raw RS gave 250 NmL CH$_4$ g^{-1} VS d. The disparity could be from the agents applied in PTM, and the employed PT RS was not exposed to biological (enzyme) hydrolysis.

Applying the modified Eq. 4 and Table 6, the chemical formula of the RS employed is C$_{761}$H$_{1336}$O$_{595}$N$_{10}$S, whilst the TBMP of the RS, calculated from Eq. 5, was 438 NmL CH$_4$ g^{-1} TS. The TBMP of 438 NmL CH$_4$ g^{-1} TS was also confirmed using the OBA™ BIOTRANSFORMERS TOOL (accessed 29 July 2022). Therefore, TBMP indicates that the methane values from the PT residues and the control are within the expected range.

Nevertheless, the actual value obtained from the raw RS (control) was significantly reduced compared to the TBMP values. The decrease in yield could be from the non-PTM of the control sample before the AD process, but in TBMP and OBA™ BIOTRANSFORMERS TOOL, RS degradation was assumed to be 100%.

The biogas yield from various PT RS residues showed that NaOH and PE-PT RS feedstocks have the highest value of 519 NmL g^{-1} TS and 487 NmL g^{-1} TS (Fig. 11). Followed by the biogas accumulation of 420 NmL g^{-1} TS recorded in HCl-PT RS reactors. On the other hand, the biogas yield of 394 NmL g^{-1} TS obtained from raw RS was almost the exact value of the SMY from NaOH-PT RS residue. The SMY of 267 NmL CH$_4$ g^{-1} TS and the cumulative biogas of 394 NmL g^{-1} TS from raw RS were within the data reported by Swedish Gas Technology Centre Ltd. (SGC)

[93] on biogas from straw. The low yield is due to the absence of both chemical and enzymatic PTM, which made the microstructure rigid and highly organised even after grinding. The mean methane content recorded in the reactors was 57% for raw RS, 60% for NaOH, 61% for PE, and 62% for HCl-PT RS residues (Fig. 11). In addition, the methane content of all the digesters stabilised to 67–70% after 5 days for NaOH, PE and HCl-PT reactors and 7 days for the raw RS fermenter, indicating that the reactors were operating well. Nonetheless, the average methane content from the various PT RS residues ranged from 68% to 70% at steady states (Fig. 12).

The a) daily specific methane production, b) daily biogas production, and c) specific methane yield from different PT RS residues after 60 d of digestion are shown in Fig. 12. The daily SMY and biogas production from the various PT RS feedstock in the continuous mode was lower than when the batch system was applied under the same environmental conditions (Fig. 11 and Fig. 12). The steady conditions were achieved between 15 and 17 d, and the result presented therein is the mean values after the steady-state was achieved. The pictograph showed that NaOH and PE-PT RS substrates gave the highest daily SMP (300 and 279 NmL CH$_4$ g^{-1} TS added d^{-1}) and daily biogas production (430 and 402 g^{-1} TS added d^{-1}), respectively, compared with values obtained for untreated RS which had daily SMP of 212 NmL CH$_4$ g^{-1} TS added d^{-1} and daily biogas production of 279 NmL g^{-1} TS added d^{-1}. Similarly, HCl-PT RS feedstock gave daily SMP of 250 NmL CH$_4$ g^{-1} TS added d^{-1} and daily biogas production of 360 NmL g^{-1} TS added d^{-1}.

Chemical and biological pretreatment of RS improved the daily SMP by 18, 31.7 and 41.5% for HCl, PE and NaOH PT RS residues than raw RS at a steady state. The daily biogas production was also improved following PTMs more than raw RS, with 53.9% for NaOH-PT RS, 43.9% for PE-PT RS, and 29% for HCl PT RS. Despite this, the result varied slightly with the percentage increment obtained by Mustafa et al. [68].

The differences in the daily SMP and biogas from NaOH and PE-PT RS, when compared to the control (raw RS), could be from the dissolution of lignin components and collapse and shrinkage of the RS cellular structures brought about by breaking of both ester, ether and β, 1–4 glucosidic bonds [60,87,89] by the chemical agents and the cellulosic enzyme. Therefore, the various PTMs exposed the RS to direct microbial attack, which ordinarily may not be possible or, even, when possible, will be time and energy-consuming.

This argument is also attested by the Gompertz model, where the methane production started approximately on day 2 when NaOH PT RS residue was employed as substrate and on day 3 when PE and HCl-PT RS residues were used (Table 11). In contrast, though the methane production started approximately 1 week after incubation when raw RS (control) was applied as a feeder, the raw RS was pretreated by reduction to 750 μm size, improving the surface area to microbial attack. As a result, the highest methane yield was obtained from day 12, which tallies with the study of Zhao et al. [108]. Additionally, the graph showed that NaOH, PE, and HCl PT-RS reactors produced higher SMY values of 16.0, 15.2, 13.0 NL, respectively, after the 60 d digestion process compared to the raw RS digesters that gave a SMY value of 10.6 NL (Fig. 12c).

3.6. Material balance of the three-stage digestion processes

The mass balance of the three-stage digestion process is presented in Fig. 13, while the corresponding purified hydrogen (m^3 H$_2$ tonne^{-1} TS) and methane (m^3 CH$_4$ tonne^{-1} TS) and the biogas yield of the different PT RS samples produced using CSABR mode are shown Table 13. For ease of tabulation and calculations, the material balance was assumed to start from 1000 g (1 kg) of raw RS. Conversely, the corresponding gases were rounded to cubic metrics per tonne (m^3 tonne^{-1}). The raw RS characterisation (Table 3) and lignocellulose composition (Fig. 2) were used for subsequent calculation for both chemical and enzymatic PTMs (see Fig. 13). However, for the stage 3 methane yield process, the analysis also included the characterisation of the individual PT RS (Table 3).
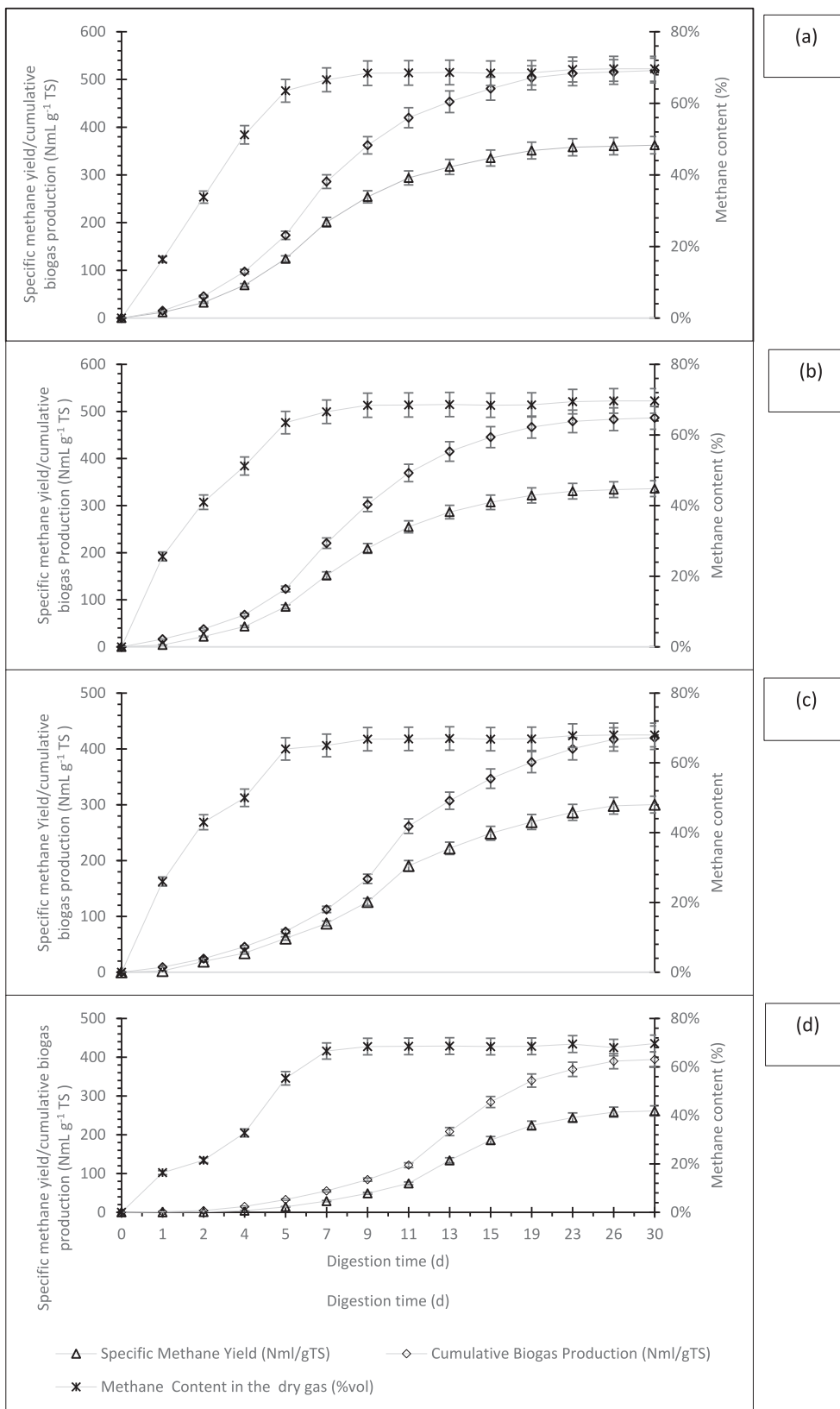
Fig. 11. Specific methane yield and cumulative biogas production from different PT RS residues ("a" NaOH, "b" PE, "c" HCl and "d" Raw (untreated) RS) using batch processes.

Table 12
Gompertz data for the batch methane production from different PT RS residues.

RS residues	Gompertz Data			
	P (NmL CH$_4$ g^{-1} TS)	λ (d)	R_m (mL d^{-1})	R-square
HCl-PT	303	2.9	23.17	0.9967
PE-PT	335	2.6	33.85	0.9992
NaOH-PT	360	1.9	38.07	0.9986
Raw (untreated)	267	6.9	22.22	0.9954

The total solids analysis was applied to estimate the TS values of the PT RS residues. Whereas the various hydrolysates, PT RS residues, raw RS and VFA effluents are considered the inputs, the methane, hydrogen, carbon dioxide and digestates were measured as the outputs. The value of lignin removed was done based on the percentage of lignin loss (Fig. 2), while the proportion of RS converted to sugars was done using the rate of enzyme conversion (Table 8).

In the acidogenic process (stage 1), the daily hydrogen production (L H$_2$ kg^{-1} TS RS) and biogas yield (L kg^{-1} TS RS) were produced from the enzymatically-PT RS hydrolysates. In contrast, the VFA effluents from the H$_2$-producing reactors were utilised to produce daily methane (L CH$_4$ kg^{-1} TS RS) and biogas (L kg^{-1} TS RS) at stage 2. After enzymatic hydrolysis, the remaining PT RS residues were used in the production of daily methane (L CH$_4$ kg^{-1} TS RS) and respective biogas (L kg^{-1} TS RS) at the stage 3 process. In the stage 3 methane fermentation, an unhydrolysed RS sample was also employed as a positive control. It is pertinent to state that the methane values recorded in Section 3.5 differed from those in Fig. 13, excluding the control sample. The disparity was because the methane values from the former (Section 3.5) were expressed in 1 g TS, unlike the latter (from mass balance), which was calculated from the RS remainders after various PTMs and lignin dissolution.
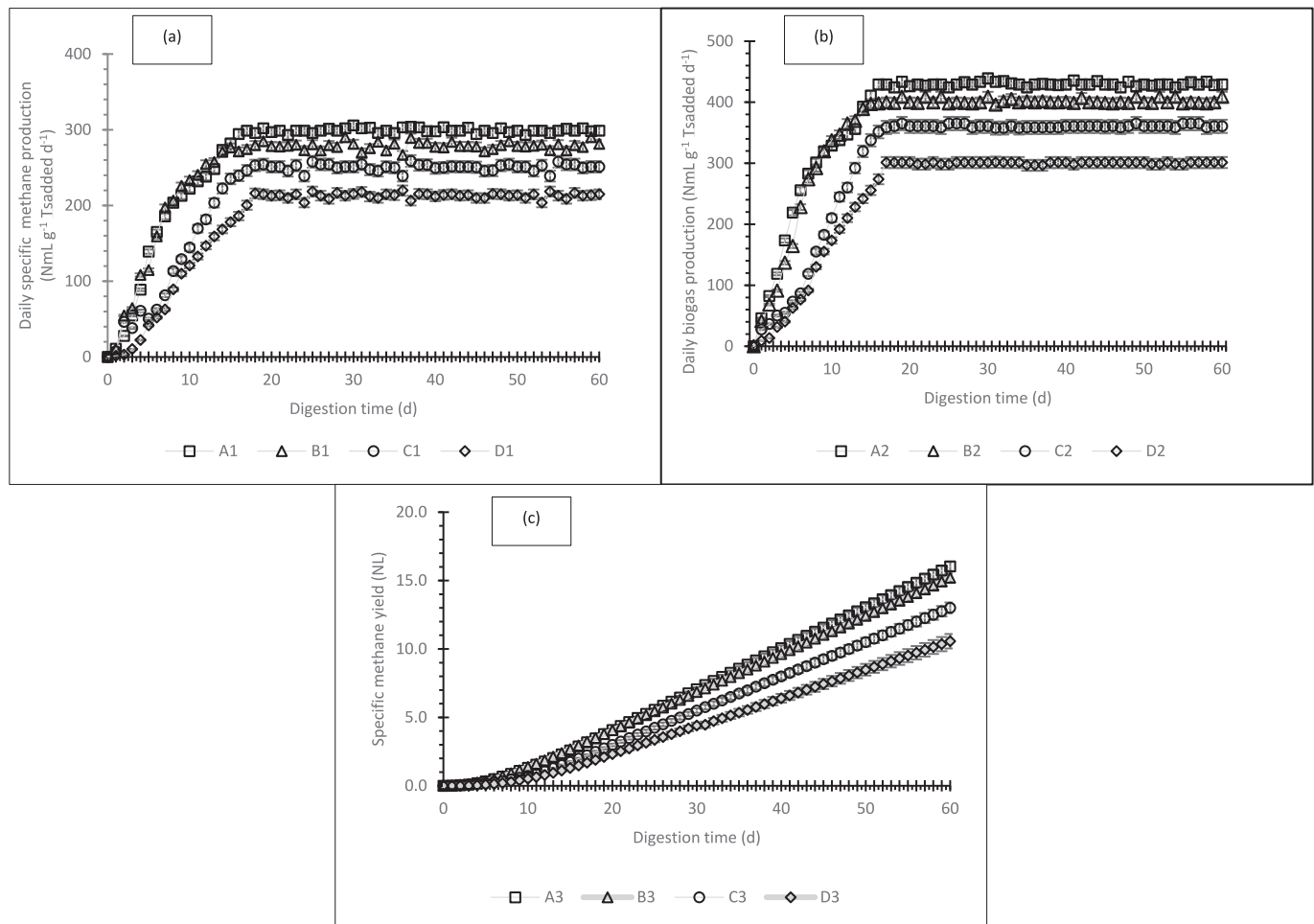
Fig. 12. The (a) daily specific methane production (NmL g^{-1} TS$_{added}$ d^{-1}), (b) daily biogas production (NmL g^{-1} TS$_{added}$ d^{-1}) and (c) specific methane yield (NL) from different PT RS residues after 60 d of digestion.
A1: Daily SMP from NaOH-PT RS residues (NmL g^{-1} TS$_{added}$ d^{-1}).
A2: Daily biogas production from NaOH-PT RS residues (NmL g^{-1} TSadded d^{-1}).
A3: SMY from NaOH-PT RS residues (NL).
B1: Daily SMP from PE-PT RS residues (NmL g^{-1} TSadded d^{-1}).
B2: Daily biogas production from PE-PT RS residues (NmL g^{-1} TSadded d^{-1}).
B3: SMY from PE-PT RS residues (NL).
C1: Daily SMP from HCl-PT RS residues (NmL g^{-1} TSadded d^{-1}).
C2: Daily biogas production from HCl-PT RS residues (NmL g^{-1} TSadded d^{-1}).
C3: SMY from HCl-PT RS residues (NL).
D1: Daily specific methane production from raw RS (NmL g^{-1} TSadded d^{-1}).
D2: Daily biogas production from raw RS (NmL g^{-1} TSadded d^{-1}).
D3: SMY from raw RS (NL).

Raw RS 1000g (1kg) per sample

Composition	(%)	Solids	(%)
Cellulose	39.5	Total solids	95
Hemi-cellulose	30.5	Volatile solids	82
Lignin	17	Ash	13
Others	13	Moisture	5

Chemical pre-treatments

Removed lignin (g)

HCl PT RS	16.15
PE PT RS	27.46
NaOH PT RS	40.38
Raw RS	N/A

RS residues (g)

HCl PT RS	933.85
PE PT RS	912.55
NaOH PT RS	909.63
Raw RS	950.00

Enzymatic Pre-treatments

RS residues converted to sugars (g)

HCl PT RS	158.75
PE PT RS	255.51
NaOH PT RS	327.47
Raw RS	76.00

RS residues (g)

HCl PT RS	775.10
PE PT RS	657.03
NaOH PT RS	582.16
Raw RS	874.00

Reducing sugar produced (g/ kg TS RS)

HCl PT RS	494.94
PE PT RS	556.65
NaOH PT RS	618.55
Raw RS	161.50

RS residues after solid analysis (g)

HCl PT RS	759.59
PE PT RS	630.75
NaOH PT RS	558.87
Raw RS	950.00

H_2 and biogas production (L/kg TS RS) using continuous systems (Stage 1) at 55°C

Acidogenic fermentation

RS samples	H_2 yield	Biogas
HCl PT RS	92	159
PE PT RS	103	179
NaOH PT RS	114	199
Raw RS	30	51

VFA effluents	gCOD/kg TS
HCl PT RS	304.24
PE PT RS	342.17
NaOH PT RS	380.22
Raw RS	99.27

RS residues converted To CH_4 (g)

HCl PT RS	432.97
PE PT RS	397.37
NaOH PT RS	363.27
Raw RS	475.00

RS digestate (g)

HCl PT RS	326.63
PE PT RS	233.38
NaOH PT RS	195.61
Raw RS	475.00

Methanogenic fermentation Stage 2

Specific CH_4 and biogas production (L CH_4/kg and L/kg TS RS) using continuous systems at 37°C

Methanogenic fermentation Stage 3

RS samles	Specific CH_4	Biogas
HCl PT RS	100	125
PE PT RS	113	141
NaOH PT RS	126	156
Raw RS	33	41

RS samples	Specific CH_4	Biogas
HCl PT RS	108	156
PE PT RS	111	160
NaOH PT RS	109	156
Raw RS	212	279

Fig. 13. RS mass balance analysis of the three-stage fermentation process from different PT technologies.

Table 13
The purified gas (H_2 and CH_4) and biogas yield from different PT RS samples using CSABR.

RS residues	Stage 1 (m³ H_2 tonne⁻¹ TS)		Stage 2 (m³ CH_4 tonne⁻¹ TS)		Stage 3 (m³ CH_4 tonne⁻¹ TS)		Total gases produced (m³ tonne⁻¹ TS)	
	Enriched	Raw	Enriched	Raw	Enriched	Raw	Enriched	Raw
HCl-PT	92	159	100	125	108	156	300	440
PE-PT	103	179	113	141	111	160	327	479
NaOH-PT	114	199	126	156	109	156	349	511
Raw	NA	NA	NA	NA	212	279	212	279

NA Not available.

The material variation in the input and output was determined using Eqs. 1 and 3 via the batch system, whereas the gases (CH_4, H_2 and biogas) produced were calculated assuming that the fermentation system was in continuous (CSABR) mode. The TS reduction/conversion to biogas used in the calculations were 57, 63, 65 and 50% for HCl, PE and NaOH-RS PT residues and raw RS, respectively. Hence, even though the TS reduction of NaOH and PE-PT RS residues coincided with Lei et al. [54] and Kim et al. [47] outcomes, there were differences in fermentation conditions and PTM methods. The higher TS reduction after PTM from NaOH and PE-PT suggests that PTM probably improved the accessibility of fermentative microorganisms for better utilisation and conversion of lignocellulose to biogas. Although the conversion values achieved were slightly higher than those obtained by Monlau et al. [64] and reported by Zieminski and Frac [110], the differences could be from the type of seed sludge and the biomass and PTM approach applied. Finally, the total gases were calculated by adding all the gases generated in all the stages for enriched (purified) gases (H_2 and CH_4) and raw biogas.

Table 13 shows the purified gas and biogas yield from different PT RS reactors via the continuous system. From the table, the PT RS samples produced the highest output of gases (purified and raw biogas) after the three-stage processes, with NaOH and PE-PT RS substrates having the highest output of 349 and 327 m³ tonne⁻¹ TS for enriched and 511 and

480 m^3 tonne^{-1} TS for raw biogas, respectively than the untreated RS which gave 212 m^3 tonne^{-1} TS as purified biogas and 279 m^3 tonne^{-1} TS as raw biogas assuming that only stage 3 process was applied. Similarly, the total gases produced from the HCl PT RS sample was 300 m^3 tonne^{-1} TS as purified biogas and 440 m^3 tonne^{-1} TS as raw biogas.

The methane production efficiency (MPE) was 80% for NaOH, 75% for PE, and 68% for HCl RS PT feedstock, while the control (raw RS) was 48%. The MPE was calculated by dividing the total purified gas (NmL CH$_4$ g^{-1} TS) produced in all the stages by the TBMP value of RS, which is 438 NmL CH$_4$ g^{-1} TS (Table 13). Pure hydrogen gas was presumed to be included in the total purified gas for the calculation.

From Table 13, the pure methane yield from stage 2 was close to those recorded in stage 3, except for the raw RS. This development could be attributed to the high methane content of raw biogas produced in stage 2 methanogenic process (Section 3.4), which is within 78–80% and requires the removal of small quantities of impurities (<20% CO$_2$) (Fig. 10). In contrast, the raw biogas from the acidogenic stage gave the highest volumetric yield in all the RS samples compared to their respective enriched biogas volume from the other stages (Table 13), which is a result of a high content of impurities (about 45% CO$_2$) which made up the volume of the produced biogas.

3.7. Energy value, electricity, and thermal generation from various RS samples

The energy values of the generated gases (purified and raw) were calculated using the data in Table 5. The H$_2$ and CH$_4$ contents were set as obtained from the literature to reflect the laboratory values, assuming that the CH$_4$ content in the raw biogas and purified gas is 70 and 99%, correspondingly. The H$_2$ content in raw biogas and purified gas is also expected to be 55 and 99%, respectively. The result of the energy value (GJ) of purified and raw biogas measured in m^3 and kg per tonne TS RS is presented in Table 14, and it is shown that the cumulative energy yield from the three-stage processes was higher from the PT samples than the raw RS supposing that only stage 3 process was applied. The highest total energy value (GJ m$^{3.1}_{biogas}$ t^{-1} TS RS) of 9.66 (25.62 GJ kg$^{-1}_{biogas}$ t^{-1} TS RS) and 9.19 (23.71 GJ kg$^{-1}_{biogas}$ t^{-1} TS RS) for purified gas and 9.00 (24.1 GJ kg$^{-1}_{biogas}$ t^{-1} TS RS) and 8.59 (22.36 GJ kg$^{-1}_{biogas}$ t^{-1} TS RS) for raw biogas were obtained from NaOH and PE PT samples respectively (Table 14). The untreated RS (control) had an energy value of 7.60 and 7.00 GJ m$^{3.1}_{biogas}$ t^{-1} TS RS (10.66 and 9.75 GJ kg$^{-1}_{biogas}$ t^{-1} TS RS) for purified and non-purified biogases, respectively, at stage 3 AD process. In the same vein, the cumulative energy value (GJ m$^{3}_{biogas}$ t^{-1} TS RS) from HCl-PT residue was 8.51 (21.57 GJ kg$^{-1}_{biogas}$ t^{-1} TS RS) for enriched and 7.98 (20.38 GJ kg$^{-1}_{biogas}$ t^{-1} TS RS) for raw biogas.

The achieved values were within the range of gross calorific value (HHV) and the raw RS sample's net energy value (LHV), determined from the oxygen bomb calorimeter and calculated using Eqs. 6, 7 and 8, which are 15.9 and 14.13 MJ kg^{-1}, respectively. The RS energy value obtained from the bomb calorimeter was validated using Dulong Eq. 14. From Dulong, an HHV of 15.5 MJ kg^{-1} for RS was achieved. The obtained values were also within the LHV of RS from the literature, ranging from 13.0 to 13.9 MJ kg^{-1} [15,62,71].

$$HHV = 337C + 1419 (H - 0.125\,O) + 93S + 23N \qquad (14)$$

Where C, H, O, S, and N are percentages of carbon, hydrogen, oxygen, sulphur, and nitrogen in RS.

Furthermore, the highest energy values measured in GJ m$^{3.1}_{biogas}$ t^{-1} TS RS were obtained from purified methane gas produced from the VFA methane reactors (stage 2) ranging from 4.07 (5.68 GJ kg$^{-1}_{biogas}$ t^{-1} TS RS) to 4.52 (6.31 GJ kg$^{-1}_{biogas}$ t^{-1} TS RS) for PE and NaOH-PT RS reactors (Table 14). On the other hand, the acidogenic process (stage 1) had the highest calorific values when measured in GJ kg$^{-1}_{biogas}$ t^{-1} TS RS for both purified and raw gases, particularly the hydrolysed samples (11.07 to 13.83). This high value in GJ kg$^{-1}_{biogas}$ t^{-1} TS RS is because hydrogen gas has a higher heating energy value of 142 MJ kg^{-1} compared to methane produced in other stages (2 and 3), which have high thermal energy of 56 MJ Kg^{-1} [14,27]. Therefore, the variations in calorific values between hydrogen and methane are critical parameters in the process comparison, as seen in Table 14, where the energy values measured in GJ m$^{3.1}_{biogas}$ t^{-1} TS RS of the raw RS are almost closer, especially with the energy values of HCl-PT RS. In contrast, the control sample's energy values (GJ kg$^{-1}_{biogas}$ t^{-1} TS RS) were approximately half of those of pre-treated RS samples. Therefore, the energy produced from PT RS samples will be more efficient, stable, and environmentally friendly than raw RS.

The electricity and thermal energy generation was done using CCHP and were determined using Table 15 and, on the postulation that data employed were from purified bio-H$_2$, that is, from the acidogenic process (stage 1), and raw biogas, that is, from the methanogenic process (stage 2 and 3). This idea is because the enriched biomethane recorded from stage 2 and 3 operations was expected to be utilised in the gas grid as a natural gas substitute. Also, it is generally believed that most CHP systems can accept small biogas impurities.

Table 15 shows the electricity and thermal energy values generated from the corresponding energy yields of the RS samples. NaOH and PE-PT RS residues gave higher electricity and thermal values than HCl-PT RS and raw RS samples. The total output energy shows that NaOH and PE-PT RS gave the most increased electricity (892.43 and 852.00 KWh$_{elect.}$ t^{-1} TS) and thermal (1194.10 and 1140.00 KWh$_{therm.}$ t^{-1} TS) values, respectively, from the three-stage processes. In contrast, the raw

Table 14
The energy value (GJ) of the purified and raw biogas per tonne of RS substrate.

RS residues	Stage 1 process (GJ m$^{3.1}_{biogas}$ t^{-1} TS)		Stage 2 process (GJ m$^{3.1}_{biogas}$ t^{-1} TS)		Stage 3 process (GJ m$^{3.1}_{biogas}$ t^{-1} TS)		Total energy (GJ m$^{3.1}_{biogas}$ t^{-1} TS)	
	Enriched	Raw	Enriched	Raw	Enriched	Raw	Enriched	Raw
HCl-PT	1.00	0.95	3.61	3.13	3.9	3.9	8.51	7.98
PE-PT	1.12	1.07	4.07	3.52	4.0	4.0	9.19	8.59
NaOH-PT	1.24	1.19	4.52	3.91	3.9	3.9	9.66	9.00
Raw	NA	NA	NA	NA	7.6	7.0	7.6	7.0

RS residues	Stage 1 process (GJ kg$^{-1}_{biogas}$ t^{-1} TS)		Stage 2 process (GJ kg$^{-1}_{biogas}$ t^{-1} TS)		Stage 3 process (GJ kg$^{-1}_{biogas}$ t^{-1} TS)		Total energy (GJ kg$^{-1}_{biogas}$ t^{-1} TS)	
	Enriched	Raw	Enriched	Raw	Enriched	Raw	Enriched	Raw
HCl-PT	11.07	10.56	5.05	4.37	5.45	5.45	21.57	20.38
PE-PT	12.45	11.87	5.68	4.91	5.58	5.58	23.71	22.36
NaOH-PT	13.83	13.19	6.31	5.46	5.48	5.45	25.62	24.10
Raw	NA	NA	NA	NA	10.66	9.75	10.66	9.75

NA Not available.

Table 15

The respective energy yields generated the electricity (KWh_elect.) and thermal energy (KWh_thermal) values.

R.S. residues	Stage 1 process (KWh t^{-1} TS)		Stage 2 process (KWh t^{-1} TS)		Stage 3 process (KWh t^{-1} TS)		Total energy (KWh t^{-1} TS)	
	Electricity	Thermal	Electricity	Thermal	Electricity	Thermal	Electricity	Thermal
HCl-PT	98.61	131.94	308.65	412.99	384.58	514.58	791.85	1059.51
PE-PT	110.44	147.78	347.11	464.44	394.44	527.78	852.00	1140.00
NaOH-PT	122.28	163.61	385.57	515.90	384.58	514.58	892.43	1194.10
Raw	NA	NA	NA	NA	690.28	923.61	690.28	923.61

NA Not available.

RS digester (control) yielded electricity and thermal values of 690.28 KWh_elect. t^{-1} TS and 923.61 KWh_therm. t^{-1} TS, respectively. Finally, the cumulative electricity and thermal yield from the HCl-PT RS source were 791.85 KWh_elect. t^{-1} TS and 1059.51 KWh_therm. t^{-1} TS.

Since Nigeria is in the tropics, most thermal energies were assumed to be employed in air conditioning, refrigeration, and cooling fluid. The heat energy was converted to cooling fluid using an absorption chiller with an outlet temperature of 6.7 °C, as defined and tabulated by the US Department of Energy [96] and Präger et al. [81]. As a result, the cooling fluid in KWh_cool produced per tonne of TS RS was 835.57, 798.00 and 741.66 for NaOH, PE and HCl PT RS samples assuming that the cooling coefficient of performance (COP) is 0.7 [96]. In addition, the cooling fluid (KWh_cool t^{-1} TS) value obtained for raw RS was 646.53. These

cooling fluids can be employed in refrigeration and chilling processes in manufacturing industries, hospitals, large commercial office buildings, cold storage warehouses and research institutes.

3.8. Microbial community analysis

The microbial configuration was examined at the end of the acidogenic and methanogenic processes, with the bacteria community's relative abundance and taxonomic distribution in each sample analysed at the genus and phylum levels (Fig. 14). However, a detailed microbial composition was discussed at the phylum level because of many unidentified Taxa at the genus level. Firmicutes were the most dominant phylum for hydrogen digesters accounting for ~85%, followed by
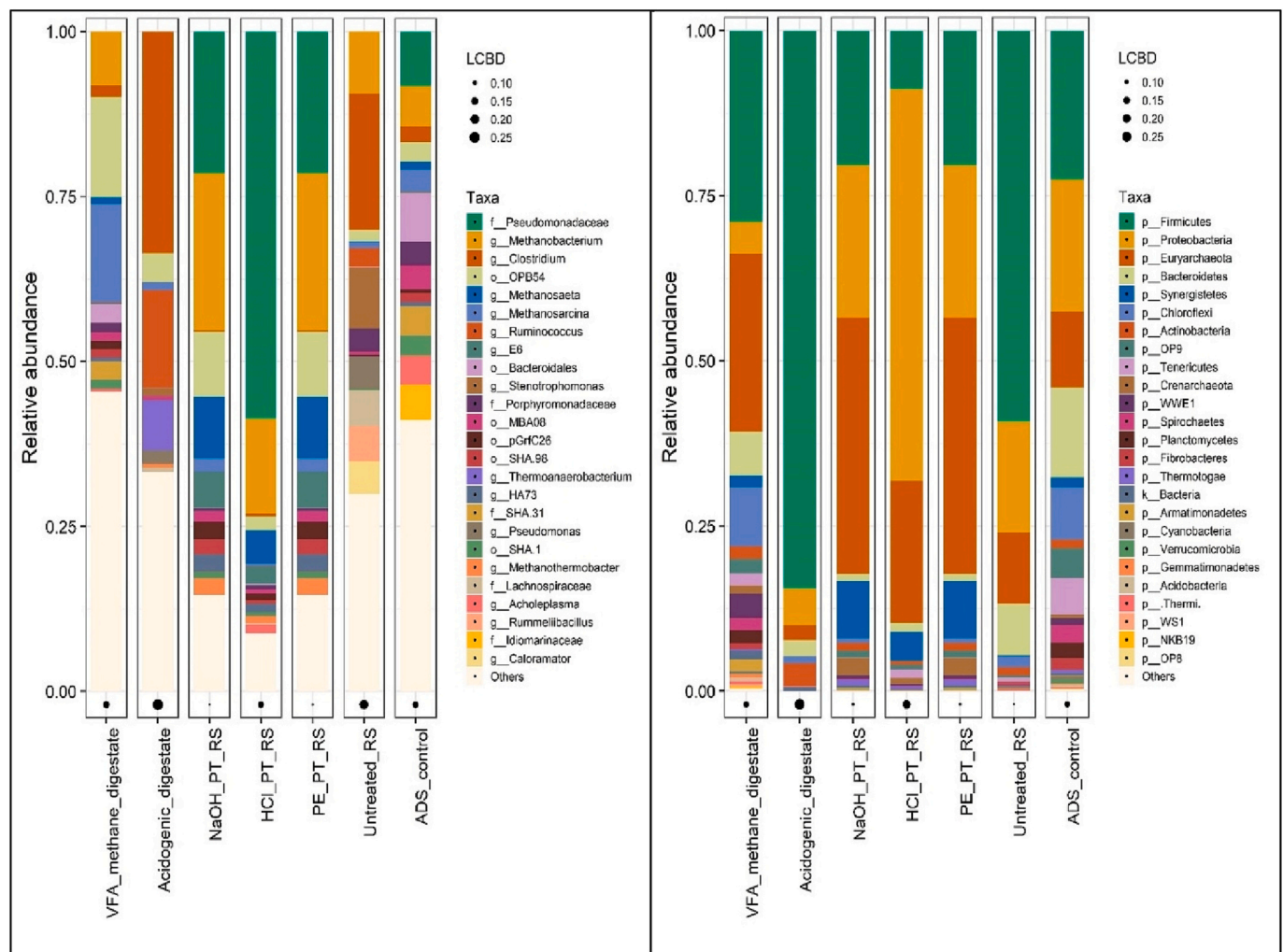
Fig. 14. The relative abundance of the 25 most abundant microbial communities at the genus and phylum levels of acidogenic and methanogenic reactors. While the bars correspond to the most dominant taxa in the sample, the black points whose diameter relates to the magnitude of the LCBD value of the digestates that is higher LCBD mean the sample has more unique species than others.

Proteobacteria and *Euryarchaeota*, which were about 5 and 4%, respectively. Others that account for ~6% of the total microbial composition were *Bacteroidetes* (~2.5%), *Actinobacteria* (~2%) and *Synergistetes* (~1%). While most of the mentioned phyla are well-known hydrogen producers from simple to complex substrates producing varying fatty acids, *Euryarchaeota* is a fastidious and strict anaerobe that produces methane using the Wood-Ljungdahl pathway (WLP). The phylum *Synergistetes* were also identified by An et al. [9] in their work on performance and energy recovery of single and two-stage biogas production from paper sludge: *Clostridium thermocellum* augmentation and microbial community analysis, where it was also reported as the significant microbial population in AD processes.

The principal phyla in the VFA digester (Stage 2) were the *Euryarchaeota* (~29%) and *Firmicutes* (~29%), followed by the *Chloroflexi* (~10%), *Bacteroidetes* (6%) and *Proteobacteria* (~3%). Other identified phyla (23%) contributed to the remaining microbial community (Fig. 14). The increased microbial population of *Firmicutes* in the SCFA digestion reactors, despite stable methane production from the phylum *Euryarchaeota,* could have been from introduction during feeding as discussed in Section 3.4. In contrast, methane production from various PT RS residues has different microbial compositions. Whereas *Euryarchaeota* (~40%) was the most abundant phylum, followed by *Proteobacteria* (~20%), *Firmicutes* (~20%) and *Synergistetes* (~9%) in NaOH and PE-PT RS digesters, *Proteobacteria* (~55%) was the dominant phylum followed by *Euryarchaeota* (~20%), *Firmicutes* (~8%) and *Synergistetes* (~3%) in HCl-PT RS digestates (Fig. 14). The existence of *Firmicutes* and *Proteobacteria* with *Euryarchaeota* in PT RS digestates is justified as their liberated product "hydrogen" is utilised in the production of methane by hydrogenotrophic methanogens of *Euryarchaeota*. Thus, in the production of methane, phyla *Firmicutes*, *Proteobacteria* and *Euryarchaeota* should exist mutually together. In addition, most *Firmicutes* are hydrolytic bacteria and are required to digest rigid RS lignocellulose to soluble derivatives such as sugars, amino acids, and fatty acids [10,45,101] essential for the growth of methanogens. However, even though *Euryarchaeota* was not the most abundant phylum in HCl-PT RS reactors, the magnitude of the LCBD value of 0.25, which represented the highest value, ensured stability in the methane production process like the other pretreated RS samples (Figs. 11 and 11). More so, it is anticipated that methane production follows the hydrogenotrophic pathway, where methane is produced via the reduction of CO_2 by H_2 produced by the *Proteobacteria* [12].

Furthermore, while the raw (untreated) RS sample had *Firmicutes* (~55%) as the most principle phylum, followed by *Proteobacteria* (~15%), *Euryarchaeota* (~12%) and *Bacteroidetes* (9%), the ADS (control) had *Firmicutes* (~23%) as the most abundant phylum, followed by *Proteobacteria* (~18%), *Bacteroidetes* (15%), *Euryarchaeota* (~12%) *Chloroflexi* (~9%), *Synergistetes* (~4%) and others (19%).

At the genus level, it can be observed from the graph that *Clostridium*, *Ruminococcus* and *Thermoanaerobacterium* were the most dominant genera and constituted most of the *Firmicutes* (Fig. 14) in the acidogenic digesters. These organisms are known hydrogen producers [58]. On the other hand, *Methanosarcina and Methanobacterium*, which constitute most of the *Euryarchaeota*, were the most abundant genera in VFA-digested reactors. While the high population of *Methanosarcina* is justified and expected as they are acetotrophic (acetoclastic) methanogens capable of utilising acetate compound (SCFA) for methane generation [12], the presence of *Methanobacterium* (though less populated compared to *Methanosarcina*) a known hydrogenotrophic methanogen is not entirely clear. However, the genus *Methanobacterium* might have been involved in methane production through the methylotrophic pathway using various C_1 compounds [12,26] contained in the VFA feedstock.

In the methane reactors from RS residues, *Methanobacterium* belonging to the phylum *Euryarchaeota,* and *Azotobacter* and *Pseudomonas* (*Pseudomonadaceae*), which belong to the phylum *Proteobacteria* were the principal genera in NaOH and PE-PT RS digestates. This is

followed by other methanogens such as *Methanosaeta*, *Methanosarcina* and *Methanothermobacter*. On the other hand, *Azotobacter* (*Pseudomonadaceae*) was the most genera in HCl-PT RS digesters, followed by *Methanobacterium* and *Methanosaeta*. As explained before, *Methanobacterium* (and *Methanothermobacter*), a hydrogenotrophic methanogen, rely on the fermentation products (H_2 and CO_2) of *Azotobacter* and *Pseudomonas* for methane production and thus explains the relative abundance in the microbial distribution mainly in the HCl-PT RS sample. However, *Methanosaeta* and *Methanosarcina* are acetotrophic (acetoclastic) methanogens. Under normal circumstances, the final phase of an AD process proceeds to methanogenesis, which involves converting C_1 methylated compounds, primarily acetate, to methane by acetotrophic methanogens [10,35], *Methanosaeta* and *Methanosarcina* would always be present in stable and efficient methane reactors.

Lastly, the raw (untreated) RS digester had *Clostridium*, a *Firmicutes,* as the most abundant genus, followed by *Methanobacterium* (*Euryarchaeota), Stenotrophomonas* and *Pseudomonas* (*Proteobacteria*). There were also a few communities of *Methanosarcina*. The complex and structural robustness of raw RS compared to PT-RS might have led to the dominancy of *Clostridium*, which is known to have hydrolytic abilities. Therefore, methane production by the methanogens is possible after RS degradation and liberation of fermentable products by *Firmicutes* and *Proteobacteria*.

4. Conclusions

This study investigated H_2 and CH_4 co-production from pretreated RS using a three-stage anaerobic digestion process with a CCHP strategy for energy generation. Experimental results showed that at the acidogenesis stage, hydrogen and biogas yield was insignificant when chemical and PE agents were employed alone. However, the daily SHP increased when the PT RS residues were biologically hydrolysed with NaOH and PE-PT PT RS residues having the highest daily SHP (114 and 103 NmL 114 NmL H_2 g^{-1} TS d^{-1}) and SMP (126 and 113 NmL CH_4 g^{-1} TS d^{-1}), respectively. Pretreated RS residues improved the daily SMY by 18–41.5% and MPE by 68–80%. The study also found that NaOH and PE-PT RS digesters produced the highest electricity and thermal yield using CCHP, with most of the heat generated being used in air conditioning, refrigeration, and cooling fluid. The cooling fluid in KWh_{cool} produced per tonne of TS RS was highest for NaOH and PE-PT RS samples. The dominant microbial communities were *Firmicutes* and *Euryarchaeota* in acidogenic and methanogenic reactors, respectively.

CRediT authorship contribution statement

Emeka Boniface Ekwenna: Writing – original draft, Visualization, Validation, Software, Methodology, Investigation, Formal analysis, Data curation, Conceptualization. **Yaodong Wang:** Writing – review & editing, Supervision. **Anthony Roskilly:** Writing – review & editing, Supervision, Resources, Project administration.

Declaration of Competing Interest

The authors declare that they have no known competing financial interests or personal relationships that could have appeared to influence the work reported in this paper.

Data availability

The authors do not have permission to share data.

References

[1] Acharya PB, Acharya DK, Modi HA. Optimisation for cellulase production by Aspergillus Niger using sawdust as substrate. Afr J Biotechnol 2008;7(22).

[2] Acharya A, Joshi DR, Shrestha K, Bhatta DR. Isolation and screening of thermophilic cellulolytic bacteria from compost piles. Sci World 2012;10(10): 43–6.

[3] Achinas S, Euverink GJW. Theoretical analysis of biogas potential prediction from agricultural waste. Resour Eff Technol 2016;2(3):143–7.

[4] Ai B, Li J, Song J, Chi X, Meng J, Zhang L, et al. Butyric acid fermentation from rice straw with undefined mixed culture: enrichment and selection of the cellulolytic butyrate-producing microbial community. Int J Agric Biol 2013;15 (6).

[5] Ajimi AN, Hammoudeh S, Nguyen DK, Sato JR. On the relationships between CO2 emissions, energy consumption and income: the importance of time variation. Energy Econ 2015;49:629–38.

[6] Akobi C, Yeo H, Hafez H, Nakhla G. Single-stage and two-stage anaerobic digestion of extruded lignocellulosic biomass. Appl Energy 2016;184:548–59.

[7] Alemahdi N, Man HC, Nasirian N, Yang Y. Enhanced mesophilic bio-hydrogen production of raw rice straw and activated sewage sludge by co-digestion. Int J Hydrogen Energy 2015;40(46):16033–44.

[8] An Q, Bu J, Cheng JR, Hu BB, Wang YT, Zhu MJ. Biological saccharification by *Clostridium thermocellum* and two-stage hydrogen and methane production from hydrogen peroxide-acetic acid pretreated sugarcane bagasse. Int J Hydrogen Energy 2020;45(55):30211–21.

[9] An Q, Cheng JR, Wang YT, Zhu MJ. Performance and energy recovery of single and two-stage biogas production from paper sludge: *Clostridium thermocellum* augmentation and microbial community analysis. Renew Energy 2020;148: 214–22.

[10] Angelidaki I, Karakashev D, Batstone DJ, Plugge CM, Stams AJM. Biomethanation and its potential. Methods Enzymol 2011;494:327–51.

[11] American Public Health Association (APHA). Standard methods for the examination of water and wastewater, 21st Eds. Water Environment Washington, DC, USA: American Public Health Association, American Water Works Association; 2005.

[12] Aryal N, Kvist T, Ammam F, Pant D, Ottosen LD. An overview of microbial biogas enrichment. Bioresour Technol 2018;264:359–69.

[13] Balachandar G, Varanasi JL, Singh V, Singh H, Das D. Biological hydrogen production via dark fermentation: A holistic approach from lab-scale to pilot-scale. Int J Hydrogen Energy 2020;45(8):5202–15.

[14] Bharathiraja B, Sudharsanaa T, Bharghav A, Jayamuthunagai J, Praveenkumar R. Biohydrogen and biogas – An overview of feedstocks and enhancement process. Fuel 2016;185:810–28.

[15] Biswas R, Pandey N, Bisht Y, Singh R, Kumar J, Bhaskar T. Pyrolysis of agricultural biomass residues: comparative study of corn cob, wheat straw, rice straw and rice husk. Bioresour Technol 2017;237:57–63.

[16] Bundhoo MZ, Mohee R. Inhibition of dark fermentative bio-hydrogen production: a review. Int J Hydrogen Energy 2016;41(16):6713–33.

[17] Bundhoo MZ, Mohee R, Hassan MA. Effects of pre-treatment technologies on dark fermentative biohydrogen production: a review. J Environ Manage 2015;157: 20–48.

[18] Cai J, Wang Y, Liu J, Zhang X, Li F. Pretreatment enhanced structural disruption, enzymatic hydrolysis, and fermentative hydrogen production from rice straw. Int J Hydrogen Energy 2022;47(23):11778–86.

[19] Callahan BJ, McMurdie PJ, Rosen MJ, Han AW, Johnson AJA, Holmes SP. DADA2: high-resolution sample inference from Illumina amplicon data. Nat Methods 2016;13(7):581–3.

[20] Callahan BJ, Sankaran K, Fukuyama JA, McMurdie PJ, Holmes SP. Bioconductor workflow for microbiome data analysis: from raw reads to community analyses. F1000Res. 2016;5(1492):1492.

[21] Caporaso JG, Kuczynski J, Stombaugh J, Bittinger K, Bushman FD, Costello EK, et al. QIIME allows the analysis of high-throughput community sequencing data. Nat Methods 2010;7(5):335–6.

[22] Chang AC, Tu YH, Huang MH, Lay CH, Lin CY. Hydrogen production by the anaerobic fermentation from acid-hydrolysed rice straw hydrolysate. Int J Hydrogen Energy 2011;36(21):14280–8.

[23] Chen CC, Chuang YS, Lin CY, Lay CH, Sen B. Thermophilic dark fermentation of untreated rice straw using mixed cultures for hydrogen production. Int J Hydrogen Energy 2012;37(20):15540–6.

[24] Cheng CL, Lo YC, Lee KS, Lee DJ, Lin CY, Chang JS. Biohydrogen production from lignocellulose feedstock. Bioresour Technol 2011;102:8514–23.

[25] Cheng J, Su H, Zhou J, Song W, Cen K. Microwave-assisted alkali pre-treatment of rice straw to promote enzymatic hydrolysis and hydrogen production in dark-and photo-fermentation. Int J Hydrogen Energy 2011;36(3):2093–101.

[26] Costa KC, Leigh JA. Metabolic versatility in methanogens. Curr Opin Biotechnol 2014;29:70–5.

[27] Das D, Veziroğlu TN. Hydrogen production by biological processes: a survey of the literature. Int J Hydrogen Energy 2001;26:13–28.

[28] Dong L, Cao G, Wu J, Liu B, Xing D, Zhao L, et al. High-solid pre-treatment of rice straw at cold temperature using NaOH/urea for enhanced enzymatic conversion and hydrogen production. Bioresour Technol 2019;287:121399.

[29] Dong L, Wu J, Zhou C, Xu CJ, Liu B, Xing D, et al. Low concentration of NaOH/ Urea pre-treated rice straw at low temperature for enhanced hydrogen production. Int J Hydrogen Energy 2020;45(3):1578–87.

[30] Du B, Sharma LN, Becker C, Chen SF, Mowery RA, van Walsum GP, et al. Effect of varying feedstock–pre-treatment chemistry combinations on the formation and accumulation of potentially inhibitory degradation products in biomass hydrolysates. Biotechnol Bioeng 2010;107(3):430–40.

[31] Edwards RL, Font-Palma C, Howe J. The status of hydrogen technologies in the UK: A multi-disciplinary review. Sust Energy Technol Assess 2021;43:100901.

[32] Food and Agriculture Organisation Corporate Statistical Database FAOSTAT (2017). http://faostat.fao.org/. (Accessed 6th May 2017).

[33] Gao J, Chen C, Lin Y, Zhang L, Ji H, Liu S. Enhanced enzymatic hydrolysis of rice straw via pretreatment with deep eutectic solvents-based microemulsions. Bioresour Technol Rep 2020;10:100404.

[34] Garba NA, Zangina U. Rice straw and husk as potential sources for mini-grid rural electricity in Nigeria. Int J Appl Sci Eng Res 2015;4(4).

[35] Gerardi MH. The microbiology of anaerobic digesters. Hoboken, New Jersey: John Wiley & Sons, Inc.; 2003.

[36] Ghimire A, Frunzo L, Pirozzi F, Trably E, Escudie R, Lens PNL, et al. A review on dark fermentative biohydrogen production from organic biomass: process parameters and use of by-products. Appl Energy 2015;144:73–95.

[37] Global Carbon Atlas (GCA) (2021). http://www.globalcarbonatlas.org/en/CO2-emissions. (Accessed 19th April 2023).

[38] He L, Huang H, Lei Z, Liu C, Zhang Z. Enhanced hydrogen production from anaerobic fermentation of rice straw pretreated by hydrothermal technology. Bioresour Technol 2014;171:145–51.

[39] Holladay JD, Hu J, King DL, Wang Y. An overview of hydrogen production technologies. Catal Today 2009;139(4):244–60.

[40] International eEnergy aAgency (IEA) (2020). https://www.iea.org/countries/nigeria#overview. [Accessed, 3rd January 2023].

[41] Jiang X, Sommer SG, Christensen KV. A review of the biogas industry in China. Energy Policy 2011;39(10):6073–81.

[42] Kainthola J, Shariq M, Kalamdhad AS, Goud VV. Enhanced methane potential of rice straw with microwave-assisted pre-treatment and its kinetic analysis. J Environ Manage 2019;232:188–96.

[43] Kannah RY, Kavitha S, Sivashanmugham P, Kumar G, Nguyen DD, Chang SW, et al. Biohydrogen production from rice straw: effect of combinative pre-treatment, modelling assessment and energy balance consideration. Int J Hydrogen Energy 2019;44(4):2203–15.

[44] Kapdan IK, Kargi F. Biohydrogen production from waste. Enzyme Microb Technol 2006;38:569–82.

[45] Khan MA, Ngo HH, Guo W, Liu Y, Zhang X, Guo J, et al. Biohydrogen production from anaerobic digestion and its potential as renewable energy. Renew Energy 2017;129:754–68.

[46] Kim DH, Jo IS, Kang BJ, Lee BD, Kumar S, Kim SH, et al. Evaluation of bio-hydrogen production using rice straw hydrolysate extracted by acid and alkali hydrolysis. Int J Hydrogen Energy 2022;47(88):37385–93.

[47] Kim M, Liu C, Noh JW, Yang Y, Oh S, Shimizu K, et al. Hydrogen and methane production from untreated rice straw and raw sewage sludge under thermophilic anaerobic conditions. Int J Hydrogen Energy 2013;38(21):8648–56.

[48] Kratky L, Jirout T. Biomass size reduction machines for enhancing biogas production. Chem Eng Technol 2011;34(3):391–9.

[49] Kshirsagar SD, Waghmare PR, Loni PC, Patil SA, Govindwar SP. Dilute acid pretreatment of rice straw, structural characterisation and optimisation of enzymatic hydrolysis conditions by response surface methodology. RSC Adv 2015;5(58):46525–33.

[50] Kumar G, Bakonyi P, Periyasamy S, Kim SH, Nemestóthy N, Bélafi-Bakó K. Lignocellulose biohydrogen: practical challenges and recent progress. Renew Sustain Energy Rev 2015;44:728–37.

[51] Kumar G, Sen B, Lin CY. Pretreatment and hydrolysis methods for recovery of fermentable sugars from de-oiled Jatropha waste. Bioresour Technol 2013;145 (1):275–9.

[52] Kumar G, Sivagurunathan P, Sen B, Mudhoo A, Davila-Vazquez G, Wang G, et al. Research and development perspectives of lignocellulose-based biohydrogen production. Int Biodeter Biodegr 2016;30:1–14.

[53] Lee DY, Ebie Y, Xu KQ, Li YY, Inamori Y. Continuous H2 and CH4 production from high-solid food waste in the two-stage thermophilic fermentation process with the recirculation of digester sludge. Bioresour Technol 2010;101(1):42–7.

[54] Lei Z, Chen J, Zhang Z, Sugiura N. Methane production from rice straw with acclimated anaerobic sludge: effect of phosphate supplementation. Bioresour Technol 2010;101(12):4343–8.

[55] Li C, Fang HPP. Fermentative hydrogen production from wastewater and solid wastes by mixed cultures. Crit Rev Environ Sci Technol 2007;37(1):1–39.

[56] Li J, Chi X, Zhang Y, Wang X. Enhanced coproduction of hydrogen and butanol from rice straw by a novel two-stage fermentation process. Int Biodeter Biodegr 2018;127:62–8.

[57] Li J, Liu W, Meng J, Zhao L, Li J, Zheng M. Mesothermal pretreatment using FeCl3 enhances methane production from rice straw. Renew Energy 2022;188:670–7.

[58] Liczbiński P, Borowski S. Effect of hyperthermophilic pretreatment on methane and hydrogen production from garden waste under mesophilic and thermophilic conditions. Bioresour Technol 2021;335:125264.

[59] Liu CM, Wu SY, Chu CY, Chou YP. Biohydrogen production from rice straw hydrolyzate in a continuously external circulating bioreactor. Int J Hydrogen Energy 2014;39(33):19317–22.

[60] Lo YC, Lu WC, Chen CY, Chang and J. S.. Dark fermentative hydrogen production from enzymatic hydrolysate of xylan and pretreated rice straw by *Clostridium butyricum* CGS5. Bioresour Technol 2010;101(15):5885–91.

[61] Lossie U, Pütz P. Targeted control of biogas plants with the help of FOS/TAC. Practice Report Hach-Lange. 2008.

[62] Maguyon-Detras MC, Migo MVP, Van Hung N, Gummert M. Thermochemical conversion of rice straw. In: Gummert M, Hung N, Chivenge P, Douthwaite B, editors. Sustainable Rice straw management. Cham, Switzerland: Springer; 2020. p. 43–64.

[63] Menardo S, Cacciatore V, Balsari P. Batch and continuous biogas production arising from feed varying in rice straw volumes following pre-treatment with extrusion. Bioresour Technol 2015;180:154–61.

[64] Monlau F, Kaparaju P, Trably E, Steyer JP, Carrere H. Alkaline pre-treatment to enhance one-stage CH4 and two-stage H2/CH4 production from sunflower stalks: mass, energy and economic balances. Chem Eng J 2015;260:377–85.

[65] Monlau F, Sambusiti C, Barakat A, Guo XM, Latrille E, Trably E, et al. Predictive models of biohydrogen and biomethane production based on the compositional and structural features of lignocellulosic materials. Environ Sci Technol 2012;46 (21):12217–25.

[66] Muñoz R, Meier L, Diaz I, Jeison D. A review on the state-of-the-art of physical/ chemical and biological technologies for biogas upgrading. Rev Environ Sci Bio/ Technol 2015;14(4):727–59.

[67] Muritala IK, Guban D, Roeb M, Sattler C. High-temperature production of hydrogen: assessment of non-renewable resources technologies and emerging trends. Int J Hydrogen Energy 2019;45(49):26022–35.

[68] Mustafa AM, Poulsen TG, Sheng K. Fungal pre-treatment of rice straw with *Pleurotus ostreatus* and *Trichoderma reese*i to enhance methane production under solid-state anaerobic digestion. Appl.Energy 2016;180:661–71.

[69] Nathao C, Sirisukpoka U, Pisutpaisal N. Production of hydrogen and methane by one and two-stage fermentation of food waste. Int J Hydrogen Energy 2013;38 (35):15764–9.

[70] Newsom C. Low-carbon approaches to tackling Nigeria's energy poverty. Renewable energy potential in Nigeria. Int Inst Environ Dev (IIED) 2012;2:45–52.

[71] Nguyen VH, Topno S, Balingbing C, Nguyen VCN, Röder M, Quilty J, et al. Generating a positive energy balance from using rice straw for anaerobic digestion. Energy Rep 2016;2:117–22.

[72] Nielsen SS. Introduction to food analysis. Food Anal 2017:3–16.

[73] Nigerian Electricity Regulatory Commission (NERC). NERC Third Quarter Report. 2018. https://nerc.gov.ng/index.php/library/documents/NERC-Reports/NE RC-Quarterly-Reports/NERC-Third-Quarter-Report-2018/. (Accessed 15th July 2020).

[74] Nigerian Energy Support Programme (NESP). The Nigerian Energy Sector. An Overview with special emphasis on renewable energy, energy efficiency and rural electrification, 2nd Edition. 2015.

[75] Oyedepo SO, Babalola OP, Nwanya SC, Kilanko O, Leramo RO, Aworinde AK, et al. Towards a sustainable electricity supply in Nigeria: the role of decentralised renewable energy system. Eur J Sustain Dev Res 2018;2(4):40.

[76] Palmqvist E, Hahn-Hägerdal B. Fermentation of lignocellulosic hydrolysates. II: inhibitors and mechanisms of inhibition. Bioresour Technol 2000;74(1):25–33.

[77] Pan CM, Ma HC, Fan YT, Hou HW. Bioaugmented cellulosic hydrogen production from cornstalk by integrating dilute acid-enzyme hydrolysis and dark fermentation. Int J Hydrogen Energy 2011;36(8):4852–62.

[78] Parawira W, Murto M, Zvauya R, Mattiasson B. Anaerobic batch digestion of solid potato waste alone and in combination with sugar beet leaves. Renew Energy 2004;29(11):1811–23.

[79] Patel SK, Kumar P, Mehariya S, Purohit HJ, Lee JK, Kalia VC. Enhancement in hydrogen production by co-cultures of Bacillus and Enterobacter. Int J Hydrogen Energy 2014;39(27):14663–8.

[80] Pöschl M, Ward S, Owende P. Evaluation of energy efficiency of various biogas production and utilisation pathways. Appl Energy 2010;87(11):3305–21.

[81] Präger F, Paczkowski S, Sailer G, Derkyi NSA, Pelz S. Biomass sources for a sustainable energy supply in Ghana–A case study for Sunyani. Ren Sust Energy Revi 2019;107:413–24.

[82] Qian DK, Geng ZQ, Sun T, Dai K, Zhang W, Zeng RJ, et al. Caproate production from xylose by mesophilic mixed culture fermentation. Bioresour Technol 2020; 308:123318.

[83] Quéméneur M, Bittel M, Trably E, Dumas C, Fourage L, Ravot G, et al. Effect of enzyme addition on fermentative hydrogen production from wheat straw. Int J Hydrogen Energy 2012;37(14):10639–47.

[84] Quéméneur M, Hamelin J, Barakat A, Steyer JP, Carrère H, Trably E. Inhibition of fermentative hydrogen production by lignocellulose-derived compounds in mixed cultures. Int J Hydrogen Energy 2012;37(4):3150–9.

[85] Ren NQ, Zhao L, Chen C, Guo WQ, Cao GL. A review on bioconversion of lignocellulosic biomass to hydrogen: key challenges and new insights. Bioresour Technol 2016;215:92–9.

[86] Rognes T, Flouri T, Nichols B, Quince C, Mahé F. VSEARCH: a versatile open-source tool for metagenomics. PeerJ 2016;4:e2584. https://doi.org/10.7717/ peerj.2584.

[87] Salakkam A, Plangklang P, Sittijunda S, Kongkeitkajorn MB, Lunprom S, Reungsang A. Bio-hydrogen and methane production from lignocellulosic materials. In: Biomass for bioenergy - recent trends and future challenges, London, UK; 2019. p. 103–42.

[88] Sambusiti C, Ficara E, Malpei F, Steyer JP, Carrère H. The benefit of sodium hydroxide pre-treatment of ensiled sorghum forage on the anaerobic reactor stability and methane production. Bioresour.Technol. 2013;144:149–55.

[89] Sattar A, Arslan C, Ji C, Sattar S, Mari IA, Rashid H, et al. Comparing the bio-hydrogen production potential of pre-treated rice straw co-digested with seeded sludge using an anaerobic bioreactor under mesophilic, thermophilic conditions. Energies 2016;9(3):198.

[90] Sen B, Chou YP, Wu SY, Liu CM. Pretreatment conditions of rice straw for simultaneous hydrogen and ethanol fermentation by mixed culture. Int J Hydrogen Energy 2016;41(7):4421–9.

[91] Srivastava N, Srivastava M, Abd-Allah EF, Singh R, Hashem A, Gupta VK. Biohydrogen production using kitchen waste as the potential substrate: A sustainable approach. Chemosphere 2021;271:129537.

[92] Ssekagiri A, Sloan W, Ijaz UZ. MicrobiomeSeq: An R package for analysis of microbial communities in an environmental context. In: ISCB Africa ASBCB conference, Kumasi, Ghana; 2017. https://github.com/umerijaz/microbiomeSeq (Vol. 10).

[93] Swedish Gas Technology Centre Ltd (SGC). Basic Data on Biogas. 2012. http://www.sgc.se/ckfinder/userfiles/files/BasicDataonBiogas2012.pdf. (Accessed on February 14th, 2020).

[94] Tabraiz S, Petropoulos E, Shamurad B, Quintela-Baluja M, Mohapatra S, Acharya K, et al. Temperature and immigration effects on quorum sensing in the biofilms of anaerobic membrane bioreactors. J Environ Manage 2021;293: 112947.

[95] Ueno Y, Fukui H, Goto M. Operation of a two-stage fermentation process producing hydrogen and methane from organic waste. Environ Sci Technol 2007; 41(4):1413–9.

[96] US Department of Energy (2017). https://www.energy.gov/sites/prod/files/ 2017/06/f35/CHP-Absorption%20Chiller-compliant.pdf. [Accessed on 8th December 2022].

[97] Usman ZG, Abbasoglu S, Ersoy NT, Fahrioglu M. Transforming the Nigerian power sector for sustainable development. Energy Policy 2015;87:429–37.

[98] Verein Deutscher Ingenieure (VDI) 4630. Fermentation of organic materials. In: Characterisation of the substrates, sampling, collection of material data, fermentation test; 2006.

[99] Wang L, Li Y, Xu L, Sun D, Wang Y, Wang Z. Rice straw pretreatment using cow breeding wastewater for methane production. Bioresour Technol 2022;346: 126657.

[100] Wei S, Zhang H, Cai X, Xu J, Fang J, Liu H. Psychrophilic anaerobic co-digestion of highland barley straw with two animal manures at high altitude for enhancing biogas production. Energ Conver Manage 2014;88:40–8.

[101] Weiland P. Biogas production: current state and perspectives. Appl Microbiol Biotechnol 2010;85(4):849–60.

[102] World Population Review. Total population by country. 2022. https://worldpop ulationreview.com/countries/nigeria-population (accessed 2nd January 2023).

[103] Yan BH, Selvam A, Wong JW. Bio-hydrogen and methane production from two-phase anaerobic digestion of food waste under the scheme of acidogenic off-gas reuse. Bioresour Technol 2020;297:122400.

[104] Yu Z, Schanbacher FL. Production of methane biogas as fuel through anaerobic digestion. In: Singh O, Harvey S, editors. Sustainable biotechnology. Dordrecht: Springer; 2010. p. 105–27.

[105] Zhang Q, Cai W. Enzymatic hydrolysis of alkali-pretreated rice straw by Trichoderma reesei ZM4-F3. Biomass Bioenergy 2008;32(12):1130–5.

[106] Zhang T, Jiang D, Zhang H, Lee DJ, Zhang Z, Zhang Q, et al. Effects of different pretreatment methods on the structural characteristics, enzymatic saccharification and photo-fermentative bio-hydrogen production performance of corn straw. Bioresour Technol 2020;304:122999.

[107] Zhang Y, Yuan J, Guo L. Enhanced bio-hydrogen production from cornstalk hydrolysate pretreated by alkaline-enzymolysis with orthogonal design method. Int J Hydrogen Energy 2020;45(6):3750–9.

[108] Zhao R, Zhang Z, Zhang R, Li M, Lei ZF, Utsumi M, et al. Methane production from rice straw pretreated by a mixture of acetic–propionic acid. Bioresour Technol 2010;101(3):990–4.

[109] Zhu H, Parker W, Basnarc R, Prorackic A, Falletta P, Berland M, et al. Biohydrogen production by anaerobic co-digestion of municipal food waste and sewage sludges. Int J Hydrogen Energy 2008;33(14):3651–9.

[110] Ziemiński K, Frąc M. Methane fermentation process as anaerobic digestion of biomass: transformations, stages and microorganisms. Afr J Biotechnol 2012;11 (18):4127–39.

[111] Udoetok IA. Characterisation of ash made from oil palm empty fruit bunches (oefb). Int. J. Environ. Sci. 2012;3(1):518–24.